Pre-print

Malusà, M. G., Danišík, M., & Kuhlemann, J. (2016).

Tracking the Adriatic-slab travel beneath the Tethyan margin of Corsica–Sardinia by low-temperature thermochronometry.

Gondwana Research, 31, 135-149.

http://dx.doi.org/10.1016/j.gr.2014.12.011

Tracking the Adriatic-slab travel beneath the Tethyan margin of Corsica-Sardinia by low-temperature thermochronometry

Marco G. Malusà [a,*], Martin Danišík [b], Joachim Kuhlemann [c]

[a] Department of Earth and Environmental Sciences, University of Milano-Bicocca, Piazza della Scienza 4, 20126 Milan, Italy

[b] Department of Earth and Ocean Sciences, University of Waikato, Private Bag 3105, Hamilton 3240, New Zealand

[c] Swiss Nuclear Safety Inspectorate, Industriestrasse 19, CH-5200 Brugg, Switzerland

*Corresponding Author: marco.malusa@unimib.it

ABSTRACT

A new multi-thermochronological dataset from Corsica-Sardinia is here employed to constrain the Meso-Cenozoic evolution of the Western Mediterranean area and the problematic transition in space and time between the opposite-dipping Alpine (European) and Apenninic (Adriatic) subductions.

The dataset, including zircon and apatite fission-track and apatite (U-Th)/He data, covers the whole Meso-Cenozoic time interval, and fits the theoretical age pattern that is expected in distal passive margins after continental break-up. This demonstrates that Corsica-Sardinia represents a fragment of the northern Tethyan margin still preserving the thermochronological fingerprint acquired during Middle Jurassic rifting. Mesozoic apatite (U-Th)/He ages from crustal sections located close to the Tethyan rift axis (i.e., central and eastern Sardinia) show that no European continental subduction took place south of Corsica since the Mesozoic. Along the Sardinia transect, post-Jurassic Adria-Europe convergence was possibly accommodated by Adriatic subduction, consistent with the onset of orogenic magmatism. In middle Eocene - Oligocene times, the northward translation of the Adriatic slab beneath the former Tethyan margin induced a coeval northward migration of erosional pulses at the surface, constrained by a trend of progressively decreasing fission track ages from southern Sardinia to NW Corsica. The Adriatic slab reached the Alpine wedge of Corsica by the end of the Oligocene without any breakoff of the European slab, and started retreating in Neogene times triggering the long-recognized basin opening in the backarc region.

Keywords: northern Tethyan margin; Alpine subduction; Apenninic subduction; slab translation; Tyrrhenian sea; Western Mediterranean.

1. Introduction

The Western Mediterranean tectonic puzzle is the result of a complex and still debated Meso-Cenozoic evolution at the boundary between the Eurasian and African plates (Dewey et al., 1989; Jolivet and Faccenna, 2000; Rosenbaum et al., 2002; Carminati et al., 2012). This plate-boundary area includes Cenozoic orogenic belts (Alps, Apennines, Betics and Pyrenées) related to different, possibly interacting, subduction zones (Jolivet et al., 2003; Vignaroli et al., 2008; Malusà et al., 2011a), and

large Neogene backarc basins (Ligurian-Provençal and Tyrrhenian) that disrupt the original relationships between these belts, thus hindering a full understanding of several crucial steps of Mediterranean evolution (Fig. 1A). Half a century since the establishment of the plate tectonic paradigm, the problematic transition in space and time between the opposite-dipping Alpine (European) and Apenninic (Adriatic) subductions (Alvarez, 1991; Molli and Malavieille 2011; Argnani, 2012), and the inferred southward extension of the Alpine orogenic wedge, are still open and heavily debated issues (Gueguen et al., 1997; Jolivet et al., 1998; Faccenna et al., 2001; Carminati et al., 2012; Turco et al., 2012; Vitale Brovarone and Herwartz, 2013). One end-member hypothesis (the so-called "young-Apennines" hypothesis, Fig. 1B) envisages the occurrence of a Cretaceous-to-Eocene Alpine subduction zone developed across the whole Western Mediterranean, later replaced, after the breakoff of the European slab, by a westward Apenninic subduction developed at the rear of the Alpine wedge since the Oligocene (e.g., Boccaletti et al., 1971; Doglioni et al., 1998; 1999; Handy et al., 2010). Another end-member hypothesis (the so-called "ancient-Apennines" hypothesis, Fig. 1B) envisages, in contrast, the occurrence of two coeval opposite-dipping subduction zones - the Alpine one to the north and the Apenninic one to the south (e.g., Principi and Treves, 1984; Rossetti et al., 2001; Argnani, 2009; Turco et al., 2012). But there is no general consensus about the location of the northern tip of the Apenninic subduction in Paleogene times (located either in front of Sardinia or in front of Corsica) and on the timing of its northward propagation (Jolivet et al., 2003; Vignaroli et al., 2008; Argnani, 2012; Advokaat et al., 2014).

The analysis of low-temperature geochronological systems in the Corsica-Sardinia continental block, a key area in terms of Alps-Apennines linkage located between the Ligurian-Provençal and Tyrrhenian basins (Fig. 1A), may provide useful data for shedding light on the timing of subduction propagation, and fundamental constraints to discriminate between the end-member reconstructions illustrated in Figure 1B. In fact, according to the ancient-Apennines hypothesis, Sardinia would be located in an upper plate position since the Mesozoic, and may thus preserve the thermochronological imprint acquired during Tethyan rifting by the distal European passive margin. According to the young-Apennines hypothesis, in contrast, Sardinia would be located in a lower plate position during most of its evolution, and the European distal margin would be no longer preserved because of subduction beneath the Adriatic plate.

In spite of its key position and the favorable widespread exposure of granites, Sardinia is relatively unexplored in terms of thermochronological work (Zattin et al., 2008). In this study, we provide the first full spatial coverage of Sardinia by three low-T thermochronometers, namely zircon and apatite fission track (ZFT and AFT), and apatite (U–Th)/He (AHe). The new data, combined with literature datasets from Corsica (e.g., Zarki-Jakni et al., 2004; Fellin et al., 2006; Danišík et al., 2007;

2012), allow us to constrain the thermal evolution of the whole Corsica-Sardinia block during rifting and subduction, in a temperature range between ~240°C and ~70°C. Results are discussed within the framework of available onshore and offshore geological constraints, providing fundamental pinpoints to the Meso-Cenozoic tectonic evolution of the Western Mediterranean area.

FIG. 1

2. Geological setting

2.1. The Corsica-Sardinia continental block

Corsica-Sardinia forms a wedge-shaped continental block largely consisting of Paleozoic rocks, with elevations exceeding 2700 m a.s.l. in NW Corsica, gradually decreasing towards the SE (Fig. 1). It preserves a complete section across the Variscan belt of southern Europe (Matte, 1991; Rossi et al., 2009), including the high-grade metamorphic rocks exposed in central Corsica and northern Sardinia (the so-called Variscan Internal Zone), and a stack of tectonic units with southward decreasing metamorphic grade exposed in southern Sardinia (P in Fig. 2). In NW Corsica, the Variscan Internal Zone is juxtaposed against Panafrican units ascribed to the Armorica microplate (P' in Fig. 2).

Upper Paleozoic magmatic rocks encased in the Variscan basement are assigned to three different magmatic associations (U1 to U3 in Fig. 2): Mg-K plutonic rocks (U1) emplaced around 340 Ma at 5-6 kbar and exclusively exposed in NW Corsica; calc-alkaline plutonic rocks (U2) emplaced around 320-290 Ma at 3-4 kbar and associated calc-alkaline volcanic rocks (U2') that are widely exposed in central-southern Corsica and Sardinia; and alkaline and metaluminous magmatic rocks (U3) emplaced around 290 Ma at <1 kbar that are exposed in northern and central Corsica (Rossi and Chocherie, 1991; Cocherie et al., 2005; Oggiano et al., 2007). Upper Paleozoic dike swarms mark inherited weakness directions within the Variscan basement (Traversa et al., 2003), where the strike of major faults ranges from NNE-SSW to NE-SW in Corsica and northern Sardinia, to N-S in southern Sardinia (Fig. 2).

Remnants of the thin Mesozoic sedimentary successions overlying the Paleozoic rocks are mainly preserved in eastern and NW Sardinia, and show great similarity, in terms of lithofacies and biofacies, with the coeval carbonate successions exposed today north of the Ligurian-Provençal basin (Azéma et al., 1977; Philip and Allemann, 1982). The Triassic – Lower Cretaceous successions (M in Fig. 2), record the typical Mesozoic evolution of the northern margin of Alpine Tethys (Lemoine et al. 1986; Fourcade et al., 1993) and include both epicontinental deposits, found in NW Sardinia, and more distal facies described on the eastern part of the island (Cherchi and Schroeder, 2002; Costamagna et al., 2007), with major Upper Triassic – Lower Jurassic stratigraphic gaps. A widespread mid-Cretaceous discontinuity is marked in NW Sardinia by bauxite deposits, formed during a period of emergence of the

Mesozoic carbonate shelf (Philip and Allemann, 1982; Busulini et al., 1984). This discontinuity is correlatable with the remnants of a Mesozoic planation surface still preserved on the Paleozoic basement of Corsica at elevations locally exceeding 2000 m a.s.l. (Rondeau, 1961; Danišík et al., 2012). Upper Cretaceous strata (K in Fig. 2) in NW Sardinia seal the wide antiformal and synformal structures deforming the underlying Mesozoic succession (Mameli et al., 2007) and include, in eastern Sardinia, minor Maastrichtian turbidites containing detrital glaucophane grains (Dieni and Massari, 1982).

Sparse Paleogene continental to shallow marine deposits lie unconformably or disconformably on the pre-Cenozoic units of the Corsica-Sardinia block (Carmignani et al., 1994; Faccenna et al., 2002). The oldest Paleogene shelf deposits are found in SE Sardinia (E1 in Fig. 2), and the coeval lignite-bearing continental deposits of SW Sardinia show angular unconformities and growth folds attesting to a syntectonic deposition (Barca and Costamagna, 2000; Dieni et al., 2008). Eocene conglomerates and Nummulitic flysch sequences (E2 in Fig. 2) are preserved on top of the Paleozoic units of Corsica (Nardi et al., 1978) and are partly accreted within a Cenozoic orogenic wedge to the NE (A1-A2 in Fig. 2) (Egal, 1992). Upper Eocene – lower Miocene conglomerates (E3 in Fig. 2) fill small syntectonic basins developed in the releasing zones of N-to-NE trending left-lateral faults (Thomas and Genneseaux, 1986; Ferrandini et al., 1999; Oggiano et al., 2009), and show local evidence of sediment cannibalization and recycling (Pasci et al., 1998). Younger continental to shallow marine deposits found in western Sardinia (N1-N2 in Fig. 2) are instead hosted in N-S half-grabens developed since the late Burdigalian, and connected by transfer zones to form an apparent N-S basin longitudinally crosscutting the entire island (Sardinia rift in Fig. 1A) (Casula et al., 2001; Oggiano et al., 2009). Cenozoic sediments are associated with widespread volcanic rocks. Orogenic volcanism (V1 in Fig. 2) has affected the western side of Sardinia since ca. 38 Ma, with a climax around 22-18 Ma, whereas anorogenic volcanic rocks (V2 in Fig. 2) were chiefly emplaced since 3 Ma (Lustrino et al., 2009).

The Cenozoic high-pressure wedge exposed in NE Corsica (Alpine Corsica in Fig. 1A; Durand-Delga, 1984; Jolivet et al., 1990; Caron, 1994) has been either associated with Alpine subduction (e.g., Mattauer et al., 1981; Malavieille et al., 1998; Vitale Brovarone et al., 2013) or with Apenninic subduction (e.g., Principi and Treves, 1984; Jolivet et al., 1998; Vitale Brovarone and Herwartz, 2013). When compared with the Western Alps, Alpine Corsica shows a similar tectonic configuration and similar timing of exhumation (Malusà et al., 2011a, and in review): tectonic units exposed in the frontal (western) part of the wedge (A2 in Fig. 2) display the oldest pressure-peak parageneses grown during Cenozoic subduction (~50 Ma in the Tenda unit; Maggi et al., 2012), and peak pressures generally lower than 1.4 GPa, whereas the youngest peak assemblages are observed on the Tyrrhenian side (~35 Ma in the Farinole-Volpajola unit, A1 in Fig. 2; Martin et al., 2011; Vitale Brovarone and Herwartz, 2013), where estimated peak pressure may largely exceed 2 GPa. As in the Western Alps,

higher-pressure units experienced very fast exhumation since ~35 Ma, and returned to the surface at rates as high as 30 km/Ma, by which time the blueschist-greenschist facies units of the frontal part of the wedge were already emplaced at shallow crustal level (Malusà et al., 2011a, and in review). For these reasons, Alpine Corsica was probably largely structured within the framework of Alpine subduction and, before the Neogene opening of the Ligurian-Provençal basin, was originally part of a continuous orogenic segment together with the Western Alps.

2.2. The Ligurian-Provençal and Tyrrhenian basins

The Corsica-Sardinia block is bounded by two Neogene basins, the Ligurian-Provençal and Tyrrhenian basins (Fig. 1A), which formed in a backarc position relative to the retreating Adriatic slab (Malinverno and Ryan, 1986; Jolivet and Faccenna, 2000). Rifting in the Ligurian-Provençal basin started in the late Oligocene, and drifting was largely coeval with the 45° counter-clockwise rotation of Corsica-Sardinia (with respect to stable Europe) constrained to between 20.5 and 15 Ma by paleomagnetic data. About 30° of Corsica-Sardinia rotation occurred between 20.5 and 18 Ma, during the climax of orogenic volcanism in Sardinia (Gattacceca et al., 2007). The crust beneath the Ligurian-Provençal basin was thinned from ~25 km to ~5 km in Neogene times, and the Moho was consequently uplifted (Bois, 1993; Chamot-Rooke et al., 1999). The continental margins, 40-50 km wide on the European side and 70-80 km wide on the Corsica-Sardinia side, show a gradual transition with the axial part of the basin, which is floored by atypical oceanic crust with discontinuous magnetic anomalies (Mauffret et al., 1995; Rollet et al., 2002). On the European margin, NE-SW normal faults (Bois, 1993; Bache et al., 2010) are parallel to the main late Variscan faults mapped onshore (e.g., the Cévennes fault; Arthaud and Seguret, 1981; Vialon, 1990). On the opposite margin, Neogene magmatism is documented north of Corsica and along the northern offshore prolongation of the Sardinia rift (Réhault et al., 2012).

The Tyrrhenian basin shows contrasting features in its northern and southern parts in terms of bathymetry, basement lithology, and Moho depth (Fig. 1A). The northern Tyrrhenian Sea is relatively shallow and has a 20-25 km deep Moho (Mauffret et al., 1999; Moeller et al., 2013; 2014) and a basement including post-Variscan metasediments, metaophiolites and limestones ascribed to a Cenozoic accretionary wedge. These rocks are unconformably overlain by Eocene to Recent deposits, exceeding 8.5 km in the Oligocene - early Miocene Corsica basin, and are intruded by upper Miocene – lower Pliocene granitoids (Colantoni et al., 1981; Mascle and Rehault, 1990; Cornamusini et al., 2002). Extension in the northern Tyrrhenian area commenced in the late Miocene and was accommodated by N-S faults, although the Corsica basin was possibly already affected by active rifting in the late Burdigalian – Langhian (Mauffret et al., 1999; Pascucci, 2002).

The southern Tyrrhenian basin is much deeper (Fig. 1A), and shows highly asymmetric conjugate margins, ~250 km wide on the Sardinian side, ~120 km wide on the southern Apennines - Calabria side

(Kastens et al., 1988). On the Sardinian margin, the upper slope hosts the ~3 km thick Sardinia basin (Sartori et al., 2004), the middle slope corresponds to the Cornaglia Terrace, a wide and rather flat area bounded to the east by the NNE-trending scarps of the Central Fault (Selli and Fabbri, 1971), and the lower part of the margin includes Plio-Quaternary oceanic areas (Sartori et al., 2004). Thick Messinian evaporites are found on the Cornaglia Terrace, which is identified as a major Messinian depocenter, but are lacking farther east (Kastens et al., 1988). The nature of the acoustic basement, which includes widespread alkaliolivinic and tholeiitic volcanic rocks, changes drastically across the Central Fault (Fig. 1A): Paleozoic continental units, locally associated with serpentinized peridotites (Baronie Seamount - Schreider et al., 1986), are exclusively found west of the Central Fault, whereas the basement east of the fault includes metasediments and metaophiolites piled up within a Cenozoic accretionary wedge (Sartori, 1986). Heat flow values are rather constant across the middle slope (120-150 mW m^{-2}), but become irregular to the east, where they show a wider range between <100 to >200 mW m^{-2} typical of young rifted domains (Della Vedova et al., 2001). Crustal thickness decreases eastward across the Cornaglia Terrace from 15-18 km to <10 km (Panza et al., 2007; Prada et al., 2014), chiefly at the expenses of the lower crust (Recq et al., 1984). Neogene extensional tectonics was diachronous across the margin: the Cornaglia Terrace was rifted from intra-Tortonian to intra-Messinian / intra-Pliocene times (Mascle and Rehault, 1990; Sartori et al., 2001), and the lower continental margin since late Tortonian times (Sartori, 1986). The upper slope was additionally affected by an earlier, poorly time-constrained extensional event, ascribed by some authors (e.g., Mascle and Rehault, 1990) to the Serravallian - early Tortonian. However, no older limit can be placed on the timing of the onset of extension in the upper and middle slope (Kastens et al., 1988) because the stratigraphic units lying beneath the upper Tortonian deep-water oozes are undated (units 5 and 6 in site 654, Fig. 1A) (Sartori et al., 1990; 2001).

FIG. 2

3. Methods

3.1. Sampling and analytical procedure

We collected 29 bedrock samples in Sardinia for AFT, ZFT and AHe analyses, at elevations ranging between 1 and >1500 m a.s.l., to provide a full spatial and vertical coverage of the whole island (Fig. 2). Most of the samples consist of Upper Paleozoic plutonic rocks (U2 in Fig. 2), locally collected directly beneath the overlying Mesozoic successions. Analyzed samples additionally include sandstones of Permian (P in Fig. 2, sample S1), Eocene (E1, sample S24), and upper Eocene - lower Burdigalian age (E3, samples S23 and S25).

Fission track analysis was carried out according to the external detector method (Gleadow, 1981), using the zeta calibration approach (Hurford and Green, 1983) and the etching protocols of Donelick et

al. (1999) for apatite, and Gleadow et al. (1976) for zircon. Horizontal confined 'tracks in tracks' were measured in *c*-axis parallel surfaces of apatite. The annealing properties of apatite were assessed by measuring D_{par} (Burtner et al., 1994). The low-T thermal history based on AFT data was modeled using the HeFTy program (Ketcham, 2005) operated with the multi-kinetic fission track annealing model of Ketcham et al. (2007), using D_{par} as a kinetic parameter and an estimator for initial track length.

Apatite crystals for (U–Th)/He analysis were hand-picked following the recommendation of Farley (2002), photographed, measured and loaded in Pt microtubes. The crystals were degassed at ~960°C under ultra-high vacuum using a diode laser, and ^{4}He was measured by isotope dilution on a Pfeiffer Prisma QMS-200 mass spectrometer. Following He measurements, the apatite crystals were spiked with ^{235}U and ^{230}Th, dissolved in nitric acid, and solutions were analyzed by isotope dilution for U and Th, and by external calibration for Sm on ICP-MS. The total analytical uncertainty, typically <5 %, was calculated as a square root of the sum of squares of uncertainty on He and weighted uncertainties on U, Th, Sm and He measurements. The raw (U–Th)/He ages were corrected for alpha ejection (Ft correction, Farley et al., 1996). A value of 5%, which is a typical precision of crystal surface and volume calculations at Waikato Thermochronology Laboratory, was adopted as the uncertainty on Ft correction and was used to calculate errors for the corrected AHe ages. Replicate analyses of internal standard Durango apatite (n = 34) measured over the period of this study, yielded mean (U–Th–Sm)/He ages of 31.3±1.9 Ma (1σ), consistent with the reference Durango (U–Th–Sm)/He age of 31.02±1.01 Ma (McDowell et al., 2005).

3.2. Conceptual thermochronological model

In order to test the end-member hypotheses illustrated in Fig. 1B, we compare the low-T geochronological age pattern observed in the study area with the theoretical age pattern expected in a distal passive margin.

In proximal passive margins, which are exposed onshore along the rim of major continents, several studies demonstrate that the temperature increase during rifting is minor (Gallagher and Brown, 1997). The thermochronological record is thus dominated by exhumation due to erosion (Brown et al., 1990; Fitzgerald, 1992; Menzies et al., 1997), and the time of break-up is recorded by an erosional response as seen in many proximal passive margins worldwide (Gallagher et al., 1994; Gleadow et al., 2002).

In distal passive margins, which are generally buried offshore beneath thick successions of post-rift sediments (e.g., Manatschal, 2004), the evidence of syn-rift sedimentation is instead supportive of a minor impact of erosion on the thermochronological record. The thermal impact of rifting could be significant due to the proximity of the rift axis, and might be quantified by low-T thermochronometry unless reset by post-rift sedimentary burial. In the light of the thermal conductivity properties of the lithosphere, however, the temperature increase during rifting is generally slow, and the effects on low-T thermochronological systems may lag by tens of millions

of years the inception of rifting (Gallagher et al., 1994; Gallagher and Brown, 1997). In Figure 3, we explore the possibility that the distal passive margin preserves the effects of such temperature increase and of the subsequent thermal re-equilibration. Re-equilibration is generally slow in the case of rift abortion (Morgan and Ramberg, 1987), but is expected to occur at much faster rates when rocks move away from the rift axis after continental break-up (Whitmarsh et al., 2001), to be potentially recorded by thermochronological systems with delays within age uncertainty. The onset of thermal relaxation may thus represent a proxy for the time of break-up.

For the sake of simplicity, the conceptual model in Figure 3 shows a more simplified thermal structure during rifting than is the real case, with rising isothermal surfaces due to asthenospheric upwelling, derived from Whitmarsh et al. (2001) that define bell-shaped areas lying at different depths according to their temperature (isotherms in the model roughly correspond to ZFT, AFT and AHe isotopic closure). Inside each half-bell, mineral ages are set during thermal relaxation after break-up at time t_B. Below the half-bell, samples are still located at temperatures higher than isotopic closure at time t_B, so that mineral ages are set during later exhumation or during younger thermal events (age < t_B). Above the half-bell, the temperature increase during rifting is not sufficient to reset the low-T thermochronological system: rocks largely preserve the thermochronological fingerprint acquired before rifting (age > t_B), but a reduction in MTL and/or a slight age rejuvenation are expected in samples that have cooled through the partial annealing (or retention) zones (red area for the AFT system in Fig. 3).

Different combinations of ZFT, AFT and AHe ages are thus expected in the distal margin according to the crustal level of each sample at the time of rifting, and according to the distance from the rift axis. For instance, indistinguishable AFT and AHe ages (= t_B) and short mean track lengths (MTL) should be found in rocks lying at shallow crustal levels and close to the rift (white circles in Fig. 3). In the real case, AHe ages may be slightly more dispersed than expected due to the complexity of radiation damage effects and crystal fragmentation (Shuster et al., 2006; Brown et al., 2013), and the thermal structure is likely more complicated due to the activity of synsedimentary faults and the differential thermal blanketing by cover rocks, which may control minor modifications in the expected first-order age pattern.

FIG. 3

4. Results

Our new dataset includes 27 new AFT ages, 7 ZFT ages, and 11 AHe ages (Fig. 4 and supplementary material). The AFT ages range between 20 and 201 Ma, and are associated with MTL between 12.2 and 13.7 μm, consistent with values reported in previous work (Fig. 4B). All of the samples passed the chi-square test, apart from two granitoid samples (S3 and S22) with $P(\chi)^2$ <5%,

yielding bimodal grain-age spectra likely due to U-zoning and inter-grain variations in Cl content (Burchart, 1981; Carlson et al., 1999) (Fig. S5). The youngest AFT ages, clustering between 20 and 22 Ma (with an additional slightly older age of 27.4 Ma), are found along a N-S belt close to the Sardinia rift (S13, S25, S26, S28, S29). The oldest AFT ages of the dataset, clustering between 169 and 201 Ma (with an additional younger age of 129 Ma), are found along the eastern coast of the island (S6, S7, S19, S20), and on the highest mountains of central Sardinia at elevations >1100 m a.s.l. (S15-S18). In this latter area, the oldest AFT ages show a normal age-elevation relationship, i.e., the age increases with elevation. The remaining AFT ages of the dataset range between 35 and 70 Ma (S1-S5, S8-S12, S14, S22-S24) and get younger from the southern part of the island towards the north.

ZFT ages are systematically older than AFT ages from the same samples and chiefly range between 195 and 239 Ma. Only one sample close to the Sardinia rift (S12), which failed the chi-square test, yielded a younger central age of 140 Ma but still shows a polymodal age distribution with a prominent age component of ~220 Ma (Fig. S5). These ZFT ages are consistent with published ZFT ages from Variscan Corsica (Fig. 2), which range between 110 and 244 Ma and only get younger close to the Alpine orogenic wedge.

AHe ages range between 21 and 204 Ma. Like the AFT dataset, the youngest ages are found close to the Sardinia rift (21-25 Ma in sample S28). The oldest ages are found on the eastern coast of the island (133-167 Ma in sample S7), and on the highest mountains of central Sardinia (148-204 Ma in sample S17). In all of these samples, the AHe ages overlap the corresponding AFT ages within error. Mesozoic AHe ages are also found in sample S16 (67-141 Ma), but are younger than the AFT age in the same sample. The remaining AHe ages fall in the range between 26-38 Ma and 57-80 Ma. They overlap (within error) the corresponding AFT ages, thus showing the same overall trend of increasing age from north to south.

FIG. 4

5. Interpretation and discussion

5.1. The thermal record of Tethyan rifting

Mesozoic low-T geochronological ages are widespread on mountain ridges of central Sardinia and on the eastern coast of the island. In these areas, AFT ages between 169 and 201 Ma, and AHe ages between 133 and 204 Ma, indicate that rocks now exposed at the surface have resided since Jurassic times at very shallow depth, i.e., above the partial annealing zone of the AFT system (~60-110°C) or even above the partial retention zone of the AHe system (~40-80°C, Stockli et al., 2000).

Within a simple interpretive framework of exhumational cooling driven by erosional removal of the overburden, the overlapping AFT and AHe ages found in samples from the eastern coast (e.g.,

169 Ma vs. 133-167 Ma in sample S7) might be interpreted as the evidence of a major Middle Jurassic erosional pulse, which induced fast exhumation across the isothermal surfaces corresponding to the closure temperatures of the AFT and AHe systems. However, this interpretation is not consistent with the compelling stratigraphic evidence of ongoing carbonate sedimentation on top of the Variscan basement during the Middle Jurassic (section 2.1).

An alternative interpretation, consistent with the model in Figure 3, can be proposed starting from the observation that these Middle Jurassic ages match the crystallization ages of trondhjemites from the Tethyan ophiolites of Alpine Corsica (161±3 and 169±3 Ma; Ohnenstetter et al., 1981; Rossi et al., 2002) and with the biostratigraphic age of the overlying radiolarites (upper Bathonian - lower Callovian; Chiari et al., 2000; Danelian et al., 2008). Similar crystallization ages are also found in many other Tethyan ophiolites now accreted in the European Alps (158–166 Ma in gabbros; Li et al., 2013). This suggests that the Mesozoic low-T geochronological ages found in eastern Sardinia were set within a tectonic framework characterized by continental rifting and oceanization. Because the first evidence of extensional faulting and differential subsidence along the future Tethyan margins are already recorded in the Late Triassic (Bertotti et al., 1993; Manatschal, 2004), isotherms had enough time to rise in the area of future break-up, in spite of the low thermal conductivity of the lithosphere. In some of the analyzed samples, resetting of the low-T geochronological systems may, therefore, have occurred because of the rising of isothermal surfaces during Tethyan rifting. Major effects of differential thermal blanketing can be excluded in the study area, because very similar thermochronological ages are found in basement samples beneath Mesozoic remnants, and in nearby areas where the Mesozoic succession is not preserved (Fig. 4).

We can thus compare our low-T geochronology dataset with the model in Figure 3, in order to infer the burial depth of different crustal sections now exposed in Corsica-Sardinia, estimate their relative distance from the Tethyan rift, and evaluate the regional trend of crust isopachs on the northern Tethyan margin during the Mesozoic (Figs. 5A,B).

Available geochronological data indicate that crustal sections now exposed in central and eastern Sardinia ($G_{1\text{-}2}$ and H in Figs. 5A,B) were originally located closer to the Tethyan rift axis than crustal sections exposed in NW Sardinia and Corsica, pointing to a NNE trend for the continental crust isopachs of the northern Tethyan margin (ENE before Corsica-Sardinia rotation). Samples from section H yielded Mesozoic AFT ages > t_B that increase with elevation from 172 Ma to 201 Ma, AHe ages range between 67 and 204 Ma, and ZFT ages range between 212 and 239 Ma. According to the model of Figure 3, the estimated Middle Jurassic overburden in section H would thus range between ~2 km and less than 1 km in samples at higher elevation, consistent with the observation that AFT and AHe ages are locally not reset by Jurassic rifting. The cooling paths

followed by these rocks inside the partial annealing zone (Fig. 6) point to geothermal gradients of >80°C/km during rifting, dropping to ~30°C/km after break-up. Samples from section G_2 yield overlapping AFT and AHe ages = t_B (169 Ma vs. 133-167 Ma), probably set during thermal relaxation after Tethyan break-up at a depth of ~2 km. The ZFT age > t_B (195 Ma) found in section G_2 confirms this interpretation, and shows that the temperature increase during rifting was not sufficient to reset the ZFT system in these rocks. Burial depth was possibly higher in block G_1, but also in this case, rocks now exposed at the surface were already well above the partial annealing zone of the ZFT system in Middle Jurassic times because ZFT ages were not reset during rifting (234 Ma).

The inferred burial depth progressively increases farther NW (Fig. 5B). ZFT ages in section F are locally partly reset, pointing to a burial depth on the order of 4-5 km, whereas the AFT and AHe systems cannot provide suitable constraints on Middle Jurassic burial because they were reset under Paleogene sediments (see chapter 5.2). A similar situation is observed in Variscan Corsica, where AFT ages are generally younger than 40 Ma and the few partly reset AFT ages, locally found on the western and southernmost part of the island, are anyway younger than 105 Ma (Zarki-Jakni et al., 2004; Fellin et al., 2005; Danišík et al., 2007). In Corsica, ZFT ages from sections D and E are generally reset by Tethyan rifting, pointing to burial depths of 6-7 km in Middle Jurassic times. In sections B_2 and C, Mesozoic burial > 7 km is suggested by ZFT ages often younger than t_B. Burial <7 km characterizes instead sections A and B_1, because ZFT ages were either set during Middle Jurassic rifting (161-165 Ma), or still preserve a Triassic – Early Jurassic geochronological fingerprint (195 to 244 Ma) (Fig. 2). These findings are consistent with the observation that rocks exposed in sections A and B_1 represent a relatively shallow crustal level, including sedimentary successions resting on Panafrican units (P' in Fig. 2) and Upper Paleozoic magmatic rocks emplaced at shallow depth (U2' and U3).

In summary, the thermal event associated with Tethyan rifting can be recognized across the whole Corsica-Sardinia block, and in different low-T geochronological systems. In eastern and central Sardinia, this thermal event is recorded by AHe and AFT data because subsequent erosion was minimal, whereas in Variscan Corsica it is recorded by ZFT data because erosion after rifting was greatest. Mesozoic post-rift erosion was rather slow, <0.1 km/Ma. In Variscan Corsica, this led to the development of a planation surface correlatable with the mid-Cretaceous bauxite deposits found in NW Sardinia and southern France, and with submarine disconformities in areas characterized by coeval marine sedimentation such as eastern Sardinia (Fig. 5C). In Alpine Corsica, the low-T geochronological evidence of Jurassic rifting was largely obliterated by Cenozoic metamorphism (ZFT ages range between 9 and 112 Ma; Mailhé et al., 1986; Cavazza et al., 2001; Zattin et al., 2001; Fellin et al., 2006), but it is still recognized in high-T systems (Rossi et al., 2002).

The model of Figure 3 may also explain the overlapping AHe and AFT ages (~20-22 Ma) and the short MTL (12.6-13.7 μm) observed along the Neogene Sardinia rift, which cuts the Tethyan isopachs at ~30° because it was largely controlled by the orientation of the retreating Adriatic trench. These ages, coeval with sedimentation in the rift and with the climax of Cenozoic magmatism, are not found far from the rift because the Corsica-Sardinia block was already exhumed at the beginning of the Neogene, and the rising isothermal surfaces could not affect surficial rocks located far from the rift axis.

FIGS. 5, 6

5.2. Cenozoic burial and exhumation

In Corsica-Sardinia, many AFT and AHe ages are clearly younger than Tethyan rifting and were not fully reset by Neogene thermal events coeval with backarc extension. These AFT ages range in Sardinia between 70 and 35 Ma (Fig. 4), whereas AHe ages in the same rocks are generally slightly younger, and sometimes overlap the corresponding AFT ages. In SW Sardinia, Paleozoic basement rocks (sample S22) yielded AFT and AHe ages of 69.9 Ma and 57-80 Ma, respectively. Similar AFT ages, but older than the stratigraphic age of analyzed rocks, are found in the overlying Cenozoic sedimentary successions (63.1 Ma in sample S23; 69.2 Ma in sample S24), and provide information on the exhumation of their parent, possibly nearby detrital sources. Younger exhumation AFT ages, between 54 and 35 Ma, are found in Paleozoic basement rocks of central and northern Sardinia, where they are associated with AHe ages ranging between 58-54 Ma and 38-26 Ma (Fig. 4). In the absence of any major thermal event between the Jurassic and the Neogene, the MTL observed in these rocks (12.2-13.4 μm) and the modeled time-temperature paths (Fig. 7) can be interpreted in terms of cooling across the partial annealing zone during erosional exhumation.

In Variscan Corsica, AFT ages chiefly range between 38 and 14 Ma (Zarki-Jakni et al., 2004; Danišík et al., 2007), with clusters around 35-30 Ma in southern Corsica and 25-20 Ma in central and northern Corsica. The occurrence of reset rocks beneath Paleogene sediments indicates that widespread AFT resetting can be ascribed to Paleogene sedimentary burial (Danišík et al., 2007). The observed MTL (12.2-14.8 μm) can thus be interpreted, like in Sardinia, in terms of cooling through the partial annealing zone during erosion of the overburden. According to Zarki-Jakni et al. (2004), erosion could be causally linked to Neogene rifting, as supported by a boomerang trend described in a set of 23 samples (but less apparent in a larger dataset of 93 samples, Fig. 4B).

However, the young AFT ages coeval with Neogene rifting are also part of a regular trend of decreasing AFT ages from southern Sardinia to northern Variscan Corsica, best observed when AFT ages are plotted along a NW-SE transect (N-S in Paleogene coordinates) (Fig. 7). MTL in the same samples show a minimum at 49 Ma, then steadily increases as AFT age decreases. This suggests a

progressively faster cooling inside the partial annealing zone moving towards the NW, as confirmed by the increasing slope in modeled cooling paths (Fig. 7). These paths also show that cooling was diachronous along the transect, inconsistent with simple tilting but instead supportive of an erosional pulse migrating northward during the Paleogene. Differential uplift and erosion of distinct fault blocks may explain the minor deviations (R=0.86) observed in this age trend.

We can, therefore, conclude that the Mesozoic planation surface was buried beneath Paleogene sediments only locally preserved in the modern landscape, and then progressively re-exposed by erosional exhumation (Fig. 8A) as described in other passive margins worldwide (e.g., Japsen et al., 2012). AFT data constrain a migrating pulse of Paleogene erosion, during which sediments were progressively removed and detritus transferred and redeposited northward on the Variscan basement. After the onset of continental subduction in Alpine Corsica, flexural subsidence on the European plate provided additional accommodation space for this detritus – including the Eocene flysch sequences of northern Corsica (E2 in Fig. 2) – and was partly accommodated by faults downthrowing the northern blocks (blocks A and B in Fig. 8).

The Mesozoic planation surface formed on top of the Variscan basement is a suitable marker for the late stages of rock uplift and tilting in the Corsica-Sardinia block (Fig. 8B). Remnants of this planation surface now dip towards the south, and are preserved at higher elevation in the NW part of the continental block. This indicates that Neogene uplift was higher in NW Corsica, where elevation now exceeds 2700 m a.s.l., and progressively decreased towards southern Corsica and Sardinia, leading to the modern wedge-shaped topographic profile shown in Fig. 1A. If such a tilting was exclusively controlled by Neogene rifting (e.g., Zarki-Jakni et al., 2004), we would expect a tilt axis parallel to the present continental margin of the Corsica-Sardinia block (i.e., a N-S tilt axis), unlike that observed. Therefore, beside Neogene rifting, the N-S variations in rock uplift observed in Corsica-Sardinia can be ascribed to lateral variations in lithospheric structure inherited from Tethyan rifting (see section 5.1), with mantle at shallow depth beneath Sardinia (as confirmed by geophysical data, Panza et al., 2007) and thicker continental crust beneath NW Corsica (Fig. 8).

FIGS. 7, 8

5.3. The linkage with offshore data

A distal position of eastern Sardinia during Tethyan rifting, here constrained on a thermochronological basis, is both consistent with the Upper Triassic – Lower Jurassic stratigraphic gaps observed onshore, which are documented in general all along the northern distal margin of the Tethys (e.g., in the Briançonnais domain of the Western Alps – Jaillard, 1985; 1989; Lemoine et al., 1986; Manatschal, 2004), and with geophysical evidence indicating no continental crust, at depth, beneath the Cornaglia Terrace (Prada et al., 2014). Such a distal position of the study area

points to the possible preservation of oceanic crust and/or exhumed subcontinental mantle offshore Sardinia, and suggests a reinterpretation of the serpentinized peridotites found on the Baronie Seamount (Schreider et al., 1986) exposed between outcrops of Variscan continental crust (Fig. 1A) and classically interpreted as the submarine extension of Alpine Corsica (e.g., Mascle and Rehault, 1990; Doglioni et al., 1999). Baronie peridotites, recovered by drilling under Miocene littoral biocalcarenites, bear no evidence of regional metamorphism and are crossed by carbonate veins with late Jurassic nannofossils, attesting their exposure on the Tethys seafloor (Schreider et al., 1986; Yasterbov et al., 1988). Noteworthy, the Baronie ridge is parallel to the NNE-trending isopachs inferred from low-T geochronology data. These rocks may represent the original subcontinental mantle exhumed during Tethyan rifting, but not involved in later subduction.

In the same way, the adjacent half-graben structures evidenced by seismic lines both in the upper slope and in the Cornaglia Terrace (Kastens et al., 1988; Prada et al., 2014) may represent an inheritance of Tethyan rifting reactivated by Neogene extension. Conglomerates drilled in clastic wedges beneath upper Tortonian deep-water oozes (site 654, Fig. 1A) include clasts of low-grade Variscan basement and clasts of lower Triassic limestones (Sartori et al., 1990), but no post-Jurassic rocks. The latter rocks are absent in conglomerates coeval with Tethyan rifting, but are exposed onshore and would, therefore, be expected in Miocene conglomerates coeval with Tyrrhenian opening. A similar evolution is suggested by the configuration of the deepest levels of the clastic wedge imaged by seismic data in the half-graben structure west of the Baronie Seamount (line GH in Prada et al., 2014, see their Fig. 5), which are affected by shortening coeval with reverse reactivation of east-dipping normal faults. This is inconsistent with simple Neogene backarc extension, but may be easily explained by inversion of Tethyan structures followed by normal reactivation during Tyrrhenian opening.

It is worth noting that Tethyan rifting was strongly asymmetrical (Lemoine et al., 1986; Manatschal, 2004). Shallow water facies were deposited on the European side of the Tethys (Caron and Gay, 1977; Jaillard, 1985; 1989) while the Adriatic margin was characterized by the deposition of deep water radiolarites (Winterer and Bosellini, 1981; Bertotti et al., 1993). Moreover, the widespread exposure of upper crustal rocks observed on the European side (Cocherie et al., 2005; Rossi et al., 2009) contrasts with the exhumation of lower crustal rocks documented on the Adriatic side (e.g., Handy and Zingg, 1991; Graessner and Schenk, 2001).

6. Implications for the Western Mediterranean evolution

6.1. Upper plate response to Adriatic slab motion

The Corsica-Sardinia block is the only area of the Western Mediterranean where evidence of Tethyan rifting is recorded by AFT and AHe data. A similar situation is observed in the basement of the Southern Alps on the upper-plate side of the Alpine subduction system, where the thermal evidence of Jurassic rifting is recorded by ZFT data (Bertotti et al., 1999). In contrast, no low-T Jurassic age is recorded, north of Corsica, on the lower plate side of the Alpine subduction system. Preservation of the low-T fingerprint acquired in Sardinia during Tethyan rifting, despite the later tectonic events in the Cretaceous (Mameli et al., 2007), Paleogene (Carmignani et al., 1994) and Neogene (Kastens et al., 1988), indicates that no European continental subduction took place south of Corsica since the Mesozoic.

Within this framework, on the Sardinia transect, the post-Jurassic Adria-Europe convergence inferred from magnetic anomalies was probably accommodated on the Adriatic side of the subduction system. Paleogene subduction of Adria beneath Sardinia is consistent with the age of the oldest Cenozoic orogenic magmatism in NW Sardinia (Lustrino et al., 2009), and with the AFT evidence of a southward tapering Alpine wedge in the Northern Apennines (Malusà and Balestrieri, 2012). The resulting Paleogene configuration of the Corsica-Sardinia area is summarized in Figure 9A, showing the trajectory of Adria relative to Europe between 67 and 23 Ma (Dewey et al., 1989) and the inferred relationships between tectonic plates in late Eocene times (35 Ma). Along the Corsica transect, Adria represents the upper plate of the choking European subduction system, where eclogite units are actively exhumed at the rear of the frontal Alpine wedge (Malusà et al., 2011a). To the south, Adriatic continental crust and Mesozoic oceanic crust are actively subducted beneath Sardinia, forming an Apenninic wedge that also includes Calabria, here interpreted as a former extensional allochthon containing slivers of lower crust. Paleocene – early Eocene convergence, accommodated along opposite-dipping subduction zones (67-49 Ma) was replaced in middle Eocene times by a progressive along-strike translation of the Adriatic slab beneath Sardinia and Corsica, which is mirrored by a coeval migration of erosional pulses at the surface (vertical arrows in Fig. 9A). We conclude that diachronous Paleogene exhumation was presumably triggered by the northward motion of Adria and by the consequent shift of the Adriatic slab beneath the remnants of the northern Tethyan margin (Fig. 9B), and that the northward-increasing erosion rates possibly mirror the interaction of the slab with progressively thicker European crust. Such an along-strike translation of the slab, also proposed recently for the western margin of North America (Pikser et al., 2012), does not require any breakoff of the European slab (Fig. 9A), but induced transpression along preexisting faults (Carmignani et al., 1994), which was replaced by extension only after the onset of Adria slab rollback in Neogene times.

FIG. 9

6.2. Meso-Cenozoic geodynamic reconstruction

Geodynamic reconstructions recently proposed within the framework of the young-Apennines hypothesis (e.g., Handy et al., 2010; Molli and Malavielle, 2011) envisage the presence of multiple spreading ridges, an almost complete consumption of relatively large microplates (e.g., AlKaPeCa in Fig. 1B), and subduction flips preceded by slab breakoff. Thermochronometry data from Corsica-Sardinia point to an alternative, straightforward reconstruction consistent with the ancient-Apennines hypothesis, as illustrated in six time frames in Figure 10.

In Middle Jurassic times, Corsica and Sardinia became part of the northern (European) distal margin of Alpine Tethys, also including windows of exhumed subcontinental mantle (BS in Fig. 10A). Both faced the Austroalpine domain, lying on the opposite (Adriatic) margin of the Tethys, and the Southalpine domain farther SW. Crustal isopachs on the passive margin were parallel to the major Variscan faults in the mainland. Adria started moving northeastward relative to Europe in Cretaceous times (Dewey et al., 1989), leading to the accretion of Austroalpine units within the Cretaceous wedge, followed by subduction of Tethyan crust beneath the Adriatic plate (Zanchetta et al., 2012). The motion of Adria was initially parallel to the northern Tethyan margin of Corsica-Sardinia (Fig. 10A), which was thus largely preserved north of the future Central Fault. The tectonic configuration south of the Central Fault is more complex, due to the transit of the Cretaceous wedge, and includes slivers of lower continental crust now exposed in Calabria. Calabria, unlike in previous reconstructions (e.g., Argnani, 2012; Turco et al., 2012), was separate from Sardinia from the early stages of Tethys opening. Tethys closure by Alpine subduction was almost completed by the latest Cretaceous (Fig. 10B).

In Paleocene – early Eocene times, eastward (Alpine) subduction propagating from the Eastern Alps was active along the Corsica transect, whereas northwestward (Apenninic) subduction was active along the Sardinia transect. East-west Adria-Europe convergence was accommodated by opposite dipping subduction zones, juxtaposed along the eastern continuation of the future Pyrenées (Fig. 10C). This scenario may additionally be supportive of northwestward subduction in the Betics, where the subduction polarity during HP metamorphism is still debated (e.g., Casas Sainz and Faccenna, 2001). A possible 45° counterclockwise rotation of the entire Corsica-Sardinia block during the Eocene, recently postulated on the basis of paleomagnetic data (Advokaat et al., 2014), represents an additional open issue, but would imply >300 km shortening between Variscan Corsica and Provence that conflicts with geological observations (Lacombe and Jolivet, 2005; Espurt et al., 2012). In the middle-late Eocene, Alpine subduction was choked and Adria started moving north-northeastward beneath the remnants of the northern Tethyan margin (Fig. 10C,D). Localized extension in the Alpine trench triggered the superfast exhumation of the Eclogite belt (Malusà et al.,

2011a) (Fig. 10D), and the Adriatic slab started its northward travel beneath Corsica, reaching the remnants of the Alpine wedge in Oligocene times. Unlike previous reconstructions that postulate slab translation beneath Corsica, but not beneath Sardinia (e.g., Argnani, 2012), the translating slab was chiefly continental (not oceanic), as confirmed by the continental basement underlying the Oligocene turbidites now accreted in the Northern Apennines (Pseudomacigno Fm; Balestrieri et al., 2011). Moreover, slab translation induced uplift and erosion on the upper plate (Fig. 9B), not orogenic collapse (cf. Argnani, 2012). Orogenic collapse in Alpine Corsica is instead ascribed to the onset of slab rollback, which induced extension in the backarc regions (Jolivet and Faccenna, 2000). Adria slab rollback led to the opening of the Ligurian-Provençal basin and to the associated Neogene counterclockwise rotation of Corsica-Sardinia (Gattacceca et al., 2007), while Adriatic foredeep turbidites were progressively accreted within the Apenninic wedge (Garzanti and Malusà, 2008) (Fig. 10E). In the late Miocene, extension east of the Corsica-Sardinia block led to the opening of the Tyrrhenian basin (Fig. 10F). Extensional reactivation affected the preexisting structures inherited from Alpine convergence offshore Corsica, and those inherited from Tethyan rifting offshore Sardinia, where the upper and middle slopes largely preserve the Mesozoic tectono-thermal imprint.

FIG. 10

7. Conclusions

Low-T geochronological data from Corsica-Sardinia unravel a Meso-Cenozoic evolution for the Western Mediterranean area summarized in the following major points:

a) Corsica-Sardinia represents a fragment of the distal northern Tethyan margin which preserves the low-T thermochronological fingerprint of Middle Jurassic rifting. The area structured during Tethyan rifting includes part of the southern Tyrrhenian basin, where peridotites exposed on the seafloor may represent windows of exhumed subcontinental mantle.

b) No evidence of Alpine continental subduction is observed south of Corsica. Along the Sardinia transect, Adria-Europe convergence was probably accommodated by subduction of Adriatic continental crust and Mesozoic oceanic crust beneath Sardinia from Paleocene times.

c) Diachronous Paleogene exhumation in Corsica-Sardinia was triggered by the progressive northward shift of the Adriatic slab beneath the remnants of the northern Tethyan margin. Adriatic-slab translation beneath the Alpine wedge of Corsica in Oligocene times did not require any breakoff of the European slab.

d) Along-strike variations in uplift of Corsica-Sardinia after Neogene rifting are explained by lateral variations in lithospheric structure inherited from Tethyan rifting. Tyrrhenian extension reactivated faults inherited from Alpine convergence offshore Corsica, and faults inherited from Tethyan rifting offshore Sardinia.

The Western Mediterranean example demonstrates that low-T thermochronological datasets provide a fundamental tool for investigating the linkage between surface and deep-seated tectonic processes, and can be successfully combined with other geological data to disentangle the evolution of complex geodynamic puzzles.

Acknowledgments

This study was funded by the German Science Foundation (DFG), projects KU 1298/3 and 1298/7, and by VEGA grant 2/0069/13. Our work benefitted from fruitful discussion with S. Baldwin, L. Crispini, A. Ellero, C. Faccenna, L. Federico, P. Fitzgerald, M.L. Frezzotti, F. Gueydan, G. Ottria, R. Polino, A. Resentini, A. Schettino, and from constructive comments by F. Rossetti and four anonymous reviewers. We thank N. Evans for English language improvement, I. Dunkl for sharing PepiFLEX software for ICP-MS data reduction, Z. Obertová for assistance with sample collection, G. Höckh, D. Mühlbayer-Renner and D. Kost for careful mineral separation.

REFERENCES

Advokaat, E.L., van Hinsbergen, D.J., Maffione, M., Langereis, C.G., Vissers, R.L., Cherchi, A., Schroeder, R., Madani, H., Columbu, S., 2014. Eocene rotation of Sardinia, and the paleogeography of the western Mediterranean region. Earth and Planetary Science Letters 401, 183-195.

Alvarez, W., 1991. Tectonic evolution of the Corsica–Apennines–Alps region studied by the method of successive approximations. Tectonics 10, 936–947.

Argnani, A., 2009. Plate tectonics and the boundary between Alps and Apennines. Italian Journal of Geosciences 128, 317-330.

Argnani, A., 2012. Plate motion and the evolution of Alpine Corsica and Northern Apennines. Tectonophysics, 579, 207-219.

Arthaud, F., Seguret, M., 1981. Les structures pyrénéennes du Languedoc et du Golfe du Lion (Sud de la France). Bulletin de la Société Géologique de France 23, 51-63.

Azéma, J., Chabrier, G., Fourcade, E., Jaffrezo, M., 1977. Nouvelles donnée micropaléontologiques, stratigraphiques et paleogeographiques sur le Portlandien et le Néocomien de Sardaigne. Revue de Micropaléontologie 20, 125-139.

Bache, F., Olivet, J.L., Gorini, C., Aslanian, D., Labails, C., Rabineau, M., 2010. Evolution of rifted continental margins: The case of the Gulf of Lions (Western Mediterranean Basin). Earth and Planetary Science Letters 292, 345–356.

Balestrieri, M.L., Pandeli, E., Bigazzi, G., Carosi, R., Montomoli, C., 2011. Age and temperature constraints on metamorphism and exhumation of the syn-orogenic metamorphic complexes of Northern Apennines, Italy. Tectonophysics 509, 254-271.

Barca, S., Costamagna, L.G., 2000. Il Bacino paleogenico del Sulcis-Iglesiente (Sardegna SW): nuovi dati stratigrafico-strutturali per un modello geodinamico nell'ambito dell'orogenesi pirenaica. Bollettino della Società Geologica Italiana 119, 497–515.

Bertotti, G., Picotti, V., Bernoulli, D., Castellarin, A., 1993. From rifting to drifting: Tectonic evolution of the south-Alpine upper crust from the Triassic to the Early Cretaceous. Sedimentary Geology 86, 53–76.

Bertotti, G., Seward, D., Wijbrans, J., Ter Voorde, M., Hurford, A.J., 1999. Crustal thermal regime prior to, during, and after rifting: A geochronological and modeling study of the Mesozoic South Alpine rifted margin. Tectonics 18, 185-200.

Bigi, G., Cosentino, D., Parotto, M., Sartori, R., Scandone, P., 1991. Structural Model of Italy, scale 1:500.000, sheet n. 5. Consiglio Nazionale delle Ricerche, Progetto Finalizzato Geodinamica, Selca, Florence (Italy).

Bigi, G., Coli, M., Cosentino, D., Dal Piaz, G.V., Parotto, M., Sartori, R., Scandone, P., 1992. Structural Model of Italy, scale 1:500.000, sheet n. 3. Consiglio Nazionale delle Ricerche, Progetto Finalizzato Geodinamica, Selca, Florence (Italy).

Boccaletti, M., Elter, P., Guazzone, G., 1971. Plate tectonic models for the development of the Western Alps and Northern Apennines. Nature 234, 108–111.

Bois, C., 1993. Initiation and evolution of the Oligo-Miocene rift basins of southwestern Europe: contribution of deep seismic reflection profiling. Tectonophysics 226, 227-252.

Brown, R.W., Rust, D.J., Summerfield, M.A., Gleadow, A.J., De Wit, M.C., 1990. An Early Cretaceous phase of accelerated erosion on the south-western margin of Africa: Evidence from apatite fission track analysis and the offshore sedimentary record. International Journal of Radiation Applications and Instrumentation. Part D. Nuclear Tracks and Radiation Measurements 17(3), 339-350.

Brown, R.W., Beucher, R., Roper, S., Persano, C., Stuart, F., Fitzgerald, P., 2013. Natural age dispersion arising from the analysis of broken crystals. Part I: Theoretical basis and implications for the apatite (U–Th)/He thermochronometer. Geochimica et Cosmochimica Acta 122, 478-497.

Burchart, J., 1981. Evaluation of uncertainties in fission-track dating: some statistical and geochemical problems. Nuclear Tracks 5, 87–92.

Burtner, R.L., Nigrini, A., Donelick, R.A., 1994. Thermochronology of Lower Cretaceous source rocks in the Idaho-Wyoming thrust belt. AAPG Bulletin 78, 1613–1636.

Busulini, A., Dieni, I., Massari, F., Pejović, D., Wiedmann, J., 1984. Nouvelles données sur le Crétacé Supérieur de la Sardaigne Orientale. Cretaceous Research 5, 243-258.

Carlson, W.D., Donelick, R.A., Ketcham, R.A. 1999. Variability of apatite fission-track annealing kinetics: I. Experimental results. American Mineralogist 84, 1213-1223.

Carmignani, L., Barca, S., Disperati, L., Fantozzi, P., Funedda, A., Oggiano, G., Pasci, S., 1994. Tertiary compression and extension in the Sardinia basement. Bollettino di Geofisica Teorica e Applicata 36, 45-62.

Carmignani, L., Rossi, P., Barca, S., Durand-Delga, M., Lahondere, D., Oggiano, G., Salvatori, I., Conti, P., Eltrudis, J., Funedda, A., Pasci, S., Cerchi, G.P., Disperati, L., Ferrandini, J., Loye-Pilot, M.D., Sartia, E., Spano, C., 2000. Carta geologica e strutturale della Sardegna e della Corsica, scala 1/500000. Servizio geologico d'Italia, Regione Sardegna, BRGM, Collectivite Territoriale de Corse.

Carminati, E., Lustrino, M., Doglioni, C., 2012. Geodynamic evolution of the central and western Mediterranean: tectonics vs. igneous petrology constraints. Tectonophysics 579, 173-192.

Caron, J.M., 1994. Metamorphism and deformation in Alpine Corsica. Schweizerische Mineralogische und Petrographische Mitteilungen 74, 105-114.

Caron, J.M., Gay, M., 1977. La couverture mésozoïque du massif d'Ambin, transition entre le domaine briançonnais et le domaine piémontais. Eclogae Geologicae Helvetiae 70, 643-665.

Casas Sainz, A.M., Faccenna, C., 2001. Tertiary compressional deformation of the Iberian plate. Terra Nova 13, 281-288.

Casula, G., Cherchi, A., Montadert, L., Muru, M., Sarria, E., 2001. The cenozoic graben system of Sardinia (Italy): geodynamic evolution from new seismic and field data. Marine and Petroleum Geology 18, 863-888.

Cavazza, W., Zattin, M., Ventura, B., Zuffa, G.G., 2001. Apatite fission-track analysis of Neogene exhumation in northern Corsica (France). Terra Nova 13, 51-57.

Chamot-Rooke, N., Gaulier, J.M., Jestin, F., 1999. Constraints on Moho depth and crustal thickness in the Liguro-Provençal basin from a 3D gravity inversion: geodynamic implications. Geological Society of London Special Publication 156, 37-61.

Cherchi, A., Schroeder, R., 2002. Jurassic and Cretaceous biostratigraphy of Nurra region (N.W. Sardinia, Italy). Paleobiogeographical remarks. Rendiconti della Società Paleontologica Italiana 1, 119-134.

Chiari, M., Marcucci, M., Principi, G., 2000. The age of radiolarian cherts associated with the ophiolites in the Apennines (Italy) and Corsica (France): a revision. Ofioliti 25, 141-146.

Cocherie, A., Rossi, P., Fanning, C.M., Guerrot, C., 2005. Comparative use of TIMS and SHRIMP for U–Pb zircon dating of A-type granites and mafic tholeiitic layered complexes and dykes from the Corsican Batholith (France). Lithos 82, 185- 219.

Colantoni, P., Fabbri, A., Gallignani, P., Sartori, R., Rehault, J.P., 1981. Carta litologica e stratigrafica dei mari italiani. Litologia Artistica Cartografica, Firenze.

Cornamusini, G., Lazzarotto, A., Merlini, S., Pascucci, V., 2002. Eocene-Miocene evolution of the north Tyrrhenian Sea. Bollettino della Società Geologica Italiana 1, 769-787.

Costamagna, L.G., Barca, S., Lecca, L., 2007. The Bajocian-Kimmeridgian Jurassic sedimentary cycle of eastern Sardinia: Stratigraphic, depositional and sequence interpretation of the new 'Baunei Group'. Comptes Rendus Geoscience 339, 601-612.

Danelian, T., De Wever, P., Durand-Delga, M., 2008. Revised radiolarian ages for the sedimentary cover of the Balagne ophiolites (Corsica, France). Implications for the palaeoenvironmental evolution of the Balano-Ligurian margin. Bulletin de la Société Géologique de France 179, 289-296.

Danišík, M., Kuhlemann, J., Dunkl, I., Székely, B., Frisch, W., 2007. Burial and exhumation of Corsica (France) in the light of fission track data. Tectonics 26(1).

Danišík, M., Kuhlemann, J., Dunkl, I., Evans, N. J., Székely, B., Frisch, W., 2012. Survival of ancient landforms in a collisional setting as revealed by combined fission track and (U-Th)/He thermochronometry: a case study from Corsica (France). Journal of Geology 120, 155-173.

Della Vedova, B., Bellani, S., Pellis, S., Squarci, P., 2001. Deep temperatures and surface heat flow distribution . In: Vai G.B., Martini I.P. (Eds.), Anatomy of an orogen: the Apennines and adjacent Mediterranean basins. Kluwer Academic Publishing, Great Britain, pp. 65-76.

Dewey, J.F., Helman, M.L., Turco, E., Hutton, D.H.W., Knott, S.D., 1989. Kinematics of the western Mediterranean, in: Coward, M.P., Dietrich, D., Park, R.G. (Eds.), Alpine tectonics. Geological Society of London Special Publication 45, pp. 265–283.

Dieni, I., Massari, F., 1982. Présence de glaucophane détritique dans le Maastrichtien inférieur de Sardaigne orientale. Comptes Rendus de l'Académie des Sciences Paris 295, 679-682.

Dieni, I., Massari, F., Médus, J., 2008. Age, depositional environment and stratigraphic value of the Cuccuru 'e Flores Conglomerate: insight into the Palaeogene to Early Miocene geodynamic evolution of Sardinia. Bulletin de la Société Géologique de France. 179, 51-72.

Doglioni, C., Mongelli, F., Pialli, G., 1998. Boudinage of the Alpine Belt in the Apenninic back-arc. Memorie della Società Geologica Italiana 52, 457–468.

Doglioni, C., Fernandez, M., Gueguen, E., Sàbat, F., 1999. On the interference between the early Apennines-Maghrebides backarc extension and the Alps-Betics orogen in the Neogene Geodvnamics of the Western Mediterranean. Bollettino della Società Geologica Italiana 118, 75-90.

Donelick, R.A., Ketcham, R.A., Carlson W.D., 1999. Variability of apatite fission-track annealing kinetics; II, Crystallographic orientation effects. American Mineralogist 84, 1224–1234.

Durand-Delga, M., 1984. Principaux traits de la Corse Alpine et corrélations avec les Alpes Ligures, Memorie della Società Geologica Italiana 28, 285–329

Egal, E., 1992. Structures and tectonic evolution of the external zone of Alpine Corsica. Journal of Structural Geology 14, 1215–1228.

Espurt, N., Hippolyte, J.C., Saillard, M., Bellier, O., 2012. Geometry and kinematic evolution of a long-living foreland structure inferred from field data and cross section balancing, the Sainte-Victoire System, Provence, France. Tectonics, 31(4).

Faccenna, C., Becker, T.W., Lucente, F.P., Jolivet, L., Rossetti, F., 2001. History of subduction and back arc extension in the Central Mediterranean. Geophysical Journal International 145, 809-820.

Faccenna, C., Speranza, F., D'Ajello Caracciolo, F., Mattei, M., Oggiano, G., 2002. Extensional tectonics on Sardinia (Italy): insights into the arc-back-arc transitional regime. Tectonophysics 356, 213-232.

Farley, K.A., 2002. (U–Th)/He dating: techniques, calibrations, and applications. Reviews in Mineralogy and Geochemistry 47, 819–844.

Farley, K.A., Wolf, R.A., Silver, L.T., 1996. The effect of long alpha-stopping distances on (U–Th)/He ages. Geochimica et Cosmochimica Acta 60, 4223–4229.

Fellin, M.G., Picotti, V., Zattin, M., 2005. Neogene to Quaternary rifting and inversion in Corsica: Retreat and collision in the western Mediterranean. Tectonics, 24(1).

Fellin, M.G., Vance, J.A., Garver, J. I., Zattin, M., 2006. The thermal evolution of Corsica as recorded by zircon fission-tracks. Tectonophysics 421, 299-317.

Ferrandini, J., Rossi, P., Ferrandini, M., Farjanel, G., Ginsburg, L., Schuler, M., Geissert, F., 1999. The Vazzio Oligocene conglomeratic formation (Ajaccio, Corsica). A record of Late Chattian synrift continental deposits in the Western Mediterranean. Comptes Rendus de l'Académie des Sciences Paris 329, 271-278.

Fitzgerald, P.G., 1992. The Transantarctic Mountains of southern Victoria Land: The application of apatite fission track analysis to a rift shoulder uplift. Tectonics, 11(3), 634-662.

Fourcade, E., Azema, J., Cecca, F., Dercourt, J., Vrielynck, B., Bellion, Y., Sandulescu, M., Ricou, L.E., 1993. Late Tithonian Palaeoenvironments (138 to 145 Ma), in: Dercourt, J., Ricou, L.E., Vriekynck, B. (Eds.), Atlas Tethys Palaeoenvironmental Maps. BEICIP-FRANLAB, Rueil-Malmaison.

Gallagher, K., Brown, R., 1997. The onshore record of passive margin evolution. Journal of the Geological Society 154(3), 451-457.

Gallagher, K., Hawkesworth, C.J., Mantovani, M.S.M., 1994. The denudation history of the onshore continental margin of SE Brazil inferred from apatite fission track data. Journal of Geophysical Research: Solid Earth 99, 18117-18145.

Garzanti, E., Malusà, M.G., 2008. The Oligocene Alps: Domal unroofing and drainage development during early orogenic growth. Earth and Planetary Science Letters, 268, 487-500.

Gattacceca, J., Deino, A., Rizzo, R., Jones, D.S., Henry, B., Beaudoin, B., Vadeboin, F., 2007. Miocene rotation of Sardinia: new paleomagnetic and geochronological constraints and geodynamic implications. Earth and Planetary Science Letters 258, 359–377.

Gleadow, A.J.W., 1981. Fission-track dating methods: What are the real alternatives? Nuclear Tracks 5, 3–14.

Gleadow, A.W.J., Hurford, A.J., Quaife, R.D., 1976. Fission track dating of zircon: improved etching techniques Earth and Planetary Science Letters 33, 273-276.

Gleadow, A.J.W., Kohn, B.P., Brown, R.W., O'Sullivan, P.B., Raza, A., 2002. Fission track thermotectonic imaging of the Australian continent. Tectonophysics, 349(1), 5-21.

Graessner, T., Schenk, V., 2001. An exposed Hercynian deep crustal section in the Sila Massif of northern Calabria: mineral chemistry, petrology and a P–T path of granulite-facies metapelitic migmatites and metabasites. Journal of Petrology 42, 931-961.

Gueguen, E., Doglioni, C., Fernandez, M., 1997. Lithospheric boudinage in the Western Mediterranean back-arc basin. Terra Nova 9, 184-187.

Handy, M.R., Zingg, A., 1991. The tectonic and rheological evolution of an attenuated cross section of the continental crust: Ivrea crustal section, southern Alps, northwestern Italy and southern Switzerland. Geological Society of America Bulletin, 103, 236-253.

Handy, M.R., Schmid, S.M., Bousquet, R., Kissling, E., Bernoulli, D., 2010. Reconciling plate-tectonic reconstructions of Alpine Tethys with the geological–geophysical record of spreading and subduction in the Alps. Earth-Science Reviews 102, 121–158.

Hurford, A.J., Green, P.F., 1983. The zeta age calibration of fission-track dating. Chemical Geology 41, 285–312.

Jaillard, E., 1985. Evolutions sédimentaire et paléotectonique de la zone briançonnaise de Vanoise occidentale (Alpes occidentales françaises). Géologie Alpine 61, 85-113.

Jaillard, E., 1989. La transition Briançonnais externe–Briançonnais interne en Savoie. L'Aiguille des Aimes, le Roc du Bourget et le massif d'Ambin. Géologie Alpine, 65, 105-134.

Japsen, P., Chalmers, J.A., Green, P.F., Bonow, J.M., 2012. Elevated, passive continental margins: Not rift shoulders, but expressions of episodic, post-rift burial and exhumation. Global and Planetary Change 90, 73-86.

Jolivet, L., Dubois, R., Fournier, M., Goffé, B., Michard, A., Jourdan, C., 1990. Ductile extension in Alpine Corsica. Geology, 18, 1007–1010.

Jolivet, L., Faccenna, C. Goffe, B., Mattei, M., Rossetti, F., Brunet, C., Storti, F., Funiciello, R., Cadet, J.P, D'Agostino, N., Parra, T., 1998. Midcrustal shear zones in postorogenic extension: example from the northern Tyrrhenian Sea. Journal of Geophysical Research: Solid Earth 103, 12123–12160.

Jolivet, L., Faccenna, C., 2000. Mediterranean extension and the Africa-Eurasia collision. Tectonics 19, 1095-1106.

Jolivet, L., Faccenna, C., Goffé, B., Burov, E., Agard, P., 2003. Subduction tectonics and exhumation of high-pressure metamorphic rocks in the Mediterranean orogens. American Journal of Science 303, 353–409.

Kastens, K.A., Mascle, J., Others, O.D.P., 1988. Leg 107 in the Tyrrhenian Sea: insights into passive margin and back-arc basin evolution. Geological Society of America Bulletin 100, 1140-1156.

Ketcham, R.A., 2005. Forward and inverse modeling of low-temperature thermochronometry data., in Reiners, P.W., Ehlers, T.A. (Eds.), Low-Temperature Thermochronology: Techniques, Interpretations, and Applications. Reviews in Mineralogy and Geochemistry 58, pp. 275–314.

Ketcham, R.A., Carter, A., Donelick, R.A., Barbarand, J., Hurford, A.J., 2007. Improved modeling of fission-track annealing in apatite. American Mineralogist 92, 799–810.

Lacombe, O., Jolivet, L., 2005. Structural relationships between Corsica and the Pyrenees-Provence domain at the time of Pyreneean orogeny, Tectonics, 24, TC1003.

Lemoine, M., Bas, T., Arnaud-Vanneau, A., Arnaud, H., Dumont, T., Gidon, M., Bourdon, M., de Graciansky, P.C., Rudkiewicz, J.L., Megard-Galli, J., Tricart, P., 1986. The continental margin of the Mesozoic Tethys in the Western Alps. Marine and Petroleum Geology 3, 179–199

Li, X.H., Faure, M., Lin, W., Manatschal, G., 2013. New isotopic constraints on age and magma genesis of an embryonic oceanic crust: the Chenaillet Ophiolite in the Western Alps. Lithos 160–161, 283–291.

Lustrino, M., Morra, V., Fedele, L., Francosi, L., 2009. Beginning of the Apennine subduction system in the central Western Mediterranean: constraints from Cenozoic orogenic magmatic activity of Sardinia, Italy. Tectonics 28, 1-23.

Maggi, M., Rossetti, F., Corfu, F., Theye, T., Andersen, T.B., Faccenna, C., 2012. Clinopyroxene–rutile phyllonites from the East Tenda Shear Zone (Alpine Corsica, France): pressure–temperature–time constraints to the Alpine reworking of Variscan Corsica. Journal of the Geological Society 169(6), 723-732.

Mailhé, D., Lucazeau, F., Vasseur, G. 1986. Uplift history of thrust belts: an approach based on fission track data and thermal modelization. Tectonophysics 124, 177–191.

Malavieille, J., Chemenda, A., Larroque, C., 1998. Evolutionary model for Alpine Corsica: mechanism for ophiolite emplacement and exhumation of high-pressure rocks, Terra Nova, 10, 317–322.

Malinverno, A., Ryan, W., 1986. Extension in the Tyrrhenian Sea and shortening in the Apennines as result of arc migration driven by sinking of the lithosphere. Tectonics 5, 227-246.

Malusà, M.G., Balestrieri, M.L., 2012. Burial and exhumation across the Alps-Apennines junction zone constrained by fission-track analysis on modern river sands. Terra Nova 24, 221-226.

Malusà, M.G., Faccenna, C., Garzanti, E., Polino, R., 2011a. Divergence in subduction zones and exhumation of high-pressure rocks (Eocene Western Alps). Earth and Planetary Science Letters 310, 21-32.

Malusà, M.G., Villa, I.M., Vezzoli, G., Garzanti, E., 2011b. Detrital geochronology of unroofing magmatic complexes and the slow erosion of Oligocene volcanoes in the Alps. Earth and Planetary Science Letters 301, 324-336.

Mameli, P., Mongelli, G., Oggiano, G., Dinelli, E., 2007. Geological, geochemical and mineralogical features of some bauxite deposits from Nurra (Western Sardinia, Italy): insights on conditions of formation and parental affinity. International Journal of Earth Sciences 96, 887-902.

Manatschal, G., 2004. New models for evolution of magma-poor rifted margins based on a review of data and concepts from West Iberia and the Alps. International Journal of Earth Sciences 93, 432-466.

Martin, L., Rubatto, D., Vitale Brovarone, A., Hermann, J. , 2011. Late Eocene lawsonite–eclogite facies metasomatism of a granulite sliver associated to ophiolites in Alpine Corsica. Lithos, 125, 620–640.

Mascle, J., Rehault, J.P., 1990. A revised seismic stratigraphy of the Tyrrhenian Sea: implications for the basin evolution, in Kastens, K.A., Mascle, J. et al. (Eds.), Proceedings of the Ocean Drilling Program, Scientific Results, vol. 107, pp. 617-636.

Mattauer, M., Faure, M., Malavieille, J., 1981. Transverse lineation and large-scale structures related to Alpine obduction in Corsica. Journal of Structural Geology 3, 401–409.

Matte, P., 1991. Accretionary history and crustal evolution of the Variscan belt in Western Europe. Tectonophysics 196, 309-337.

Mauffret, A., Pascal, G., Maillard, A., Gorini, C., 1995. Tectonics and deep structure of the north-western Mediterranean Basin. Marine and Petroleum Geology 12, 645-666.

Mauffret, A., Contrucci, I., Brunet, C., 1999. Structural evolution of the Northern Tyrrhenian Sea from new seismic data. Marine and Petroleum Geology 16, 381-407.

McDowell, F.W., McIntosh, W.C., Farley, K.A., 2005. A precise ^{40}Ar-^{39}Ar reference age for the Durango apatite (U–Th)/He and fission track dating standard. Chemical Geology 214, 249-263.

Menzies, M., Gallagher, K., Yelland, A., Hurford, A.J., 1997. Volcanic and nonvolcanic rifted margins of the Red Sea and Gulf of Aden: crustal cooling and margin evolution in Yemen. Geochimica et Cosmochimica Acta, 61(12), 2511-2527.

Moeller, S., Grevemeyer, I., Ranero, C.R., Berndt, C., Klaeschen, D., Sallares, V., Zitellini, N., de Franco, R., 2013. Early-stage rifting of the northern Tyrrhenian Sea Basin: Results from a combined wide-angle and multichannel seismic study. Geochemistry, Geophysics, Geosystems, 14(8), 3032-3052.

Moeller, S., Grevemeyer, I., Ranero, C.R., Berndt, C., Klaeschen, D., Sallares, V., Zitellini, N., de Franco, R., 2014. Crustal thinning in the northern Tyrrhenian Rift: Insights from multichannel and wide-angle seismic data across the basin. Journal of Geophysical Research: Solid Earth, 119(3), 1655-1677.

Molli, G., Malavieille, J., 2011. Orogenic processes and the Corsica/Apennines geodynamic evolution: insights from Taiwan. International Journal of Earth Sciences 100, 1207-1224.

Morgan, P., Ramberg, I.B., 1987. Physical changes in the lithosphere associated with thermal relaxation after rifting. Tectonophysics 143, 1-11.

Nardi, R., Puccinelli, A., Verani, M., 1978. Carta geologica della Balagne “sedimentaria” (Corsica) alla scala 1:25.000 e note illustrative. Bollettino della Società Geologica Italiana 97, 11-30.

Oggiano, G., Casini, L., Rossi, P., Mameli, P., 2007. Long lived dextral strike-slip tectonics in the Southern Variscan Belt: evidences from two synkynematic intrusions of North Sardinia (Italy). Géologie de la France 2, 141.

Oggiano, G., Funedda, A., Carmignani, L., Pasci, S., 2009. The Sardinia-Corsica microplate and its role in the Northern Apennine geodynamics: new insights from the Tertiary intraplate strike-slip tectonics of Sardinia. Italian Journal of Geosciences 128, 527-539.

Ohnenstetter, M., Ohnenstetter, D., Vidal, P., Cornichet, J., Hermitte, D., Mace, J., 1981. Crystallization and age of zircon from Corsican ophiolitic albitites: consequences for oceanic expansion in Jurassic time. Earth and Planetary Science Letters 54, 397-408.

Panza, G.F., Peccerillo, A., Aoudia, A., Farina, B., 2007. Geophysical and petrological modelling of the structure and composition of the crust and upper mantle in complex geodynamic settings: the Tyrrhenian Sea and surroundings. Earth-Science Reviews 80, 1-46.

Pasci, S., Oggiano, G., Funedda, A., 1998. Rapporti tra tettonica e sedimentazione lungo le fasce trascorrenti Oligo-Aquitaniane della Sardegna NE. Bollettino della Società Geologica Italiana 117, 443-453.

Pascucci, V., 2002. Tyrrhenian Sea extension north of the Elba Island between Corsica and western Tuscany (Italy). Bollettino della Società Geologica Italiana 1, 819-828.

Philip, J., Allemann, J., 1982. Comparaison entre les plates-formes du Crétacé Supérieur de Provence and Sardaigne. Cretaceous Research 3, 35-45.

Pikser, J.E., Forsyth, D.W., Hirth, G., 2012. Along-strike translation of a fossil slab. Earth and Planetary Science Letters 331–332, 315–321.

Prada, M., Sallarès, V., Ranero, C. R., Vendrell, M. G., Grevemeyer, I., Zitellini, N., de Franco, R., 2014. Seismic structure of the Central Tyrrhenian basin: Geophysical constraints on the nature of the main crustal domains. Journal of Geophysical Research: Solid Earth, 119(1), 52-70.

Principi, G., Treves, B., 1984. Il sistema corso-appenninico come prisma d'accrezione. Riflessi sul problema generale del limite Alpi-Appennino. Memorie della Società Geologica Italiana 28, 549–576.

Recq, M., Rehault, J.P., Steinmetz, L., Fabbri, A., 1984. Amincissement de la croute et accretion au centre du bassin Tyrrhenien d’aprés la sismique refraction. Marine Geology 55, 411-428.

Réhault, J.P., Honthaas, C., Guennoc, P., Bellon, H., Ruffet, G., Coten, J., Sosson, M., Maury, R.C., 2012. Offshore Oligo-Miocene volcanic fields within the Corsica-Liguria Basin: magmatic diversity and slab evolution in the western Mediterranean Sea. Journal of Geodynamics 58, 73-95.

Rollet, N., Déverchère, J., Beslier, M.O., Guennoc, P., Réhault, J.P., Sosson, M., Truffert, C., 2002. Back arc extension, tectonic inheritance, and volcanism in the Ligurian Sea, Western Mediterranean. Tectonics 21, 1-23.

Rondeau, A. 1961. Recherches géomorphologiques en Corse (la part de la téctonique et de l’érosion differentielle dans le relief de l’île). Monographie, 586 p.

Rosenbaum, G., Lister, G.S., Duboz, C., 2002. Reconstruction of the tectonic evolution of the western Mediterranean since the Oligocene. Journal of the Virtual Explorer 8, 107-130.

Rossetti, F., Faccenna, C., Goffé, B., Monié, P., Argentieri, A., Funiciello, R., Mattei, M., 2001. Alpine structural and metamorphic signature of the Sila Piccola Massif nappe stack (Calabria, Italy): Insights for the tectonic evolution of the Calabrian Arc. Tectonics 20, 112-133.

Rossi, P., Cocherie, A., 1991. Genesis of a Variscan Batholith. Field, petrological and mineralogical evidence from the Corsica-Sardinia batholith. Tectonophysics 195, 319– 346.

Rossi, P., Cocherie, A., Lahondere, D., Fanning, M., 2002. La marge européenne de la Téthys jurassique an Corse. datation de trondhjémites de Balagne at indices de croûte continentale sous le domaine Balano-Ligure. Comptes Rendus Geoscience 334, 313-322.

Rossi, P., Oggiano, G., Cocherie, A., 2009. A restored section of the "southern Variscan realm" across the Corsica-Sardinia microcontinent. Comptes Rendus Geoscience 341, 224-238.

Sartori, R., 1986. Notes on the geology of the acoustic basement in the Tyrrhenian sea. Memorie della Società Geologica Italiana 36, 99-108.

Sartori, R., Mascle, G., Bouillin, J.P., Girault, J., Naud, G., Pasini, M., Piboule, M., 1990. Types and sources of large rock clasts and of heavy minerals from ODP sites 652, 653, 654, and 656 in the Tyrrhenian Sea: implications about the nature of the east Sardinia passive continental margin, in: Kastens K.A., Mascle J. et al. (Eds.), Proceedings of the Ocean Drilling Program, Scientific Results, vol. 107, pp. 29-35.

Sartori, R., Carrara, G., Torelli, L., Zitellini, N., 2001. Neogene evolution of the southwestern Tyrrhenian Sea (Sardinia Basin and western bathyal plain). Marine Geology 175, 47-66.

Sartori, R., Torelli, L., Zitellini, N., Carrara, G., Magaldi, M., Mussoni, P., 2004. Crustal features along a W-E Tyrrhenian transect from Sardinia to Campania margins (Central Mediterranean). Tectonophysics 383, 171-192.

Schreider, A.A., Yastrebov, V.S., Rimsky-Korsakov, N.A., Savelli, C., 1986. Indagini e campionature di dettaglio di affioramenti rocciosi submarini dei Monti Baronie (Mar Tirreno): primi risultati. Memorie della Società Geologica Italiana 36, 91-98.

Selli, R., Fabbri, A., 1971. Tyrrhenian: a Pliocene deep-sea. Atti dell'Accademia Nazionale dei Lincei, Rendiconti 50, 580-592.

Shuster, D.L., Flowers, R.M., Farley, K.A., 2006. The influence of natural radiation damage on helium diffusion kinetics in apatite. Earth and Planetary Science Letters 249, 148-161.

Stockli, D.F., Farley, K.A., Dumitru, T.A., 2000. Calibration of the apatite (U-Th)/He thermochronometer on an exhumed fault block, White Mountains, California. Geology 28, 983-986.

Thomas, B., Gennesseaux, M., 1986. A two stage rifting in the basin of the Corsica-Sardinia strait. Marine Geology 72, 225-239.

Traversa, G.B., Ronca, S., Del Moro, A., Pasquali, C., Buraglini, N., Barabino, G.C., 2003. Late to post-Hercynian dyke activity in the Sardinia-Corsica Domain: a transition from orogenic calc-alkaline to anorogenic alkaline magmatism. Bollettino della Società Geologica Italiana 2, 131-152.

Turco, E., Macchiavelli, C., Mazzoli, S., Schettino, A., Pierantoni, P.P., 2012. Kinematic evolution of Alpine Corsica in the framework of Mediterranean mountain belts. Tectonophysics 579, 193-206.

Yastrebov, V.S., Savelli, C., Sborshchikov, I., Schreider, A.A., 1988. On the oceanic crust of the Tyrrhenian Sea: present knowledge and open problems. Memorie della Società Geologica Italiana 41, 547-556.

Vialon, P., 1990. Deep Alpine structures and geodynamic evolution: an introduction and outline of a new interpretation. Mémoires de la Société Géologique de France 156, 7-14.

Vignaroli, G., Faccenna, C., Jolivet, L., Piromallo, C., Rossetti, F., 2008. Subduction polarity reversal at the junction between the Western Alps and the Northern Apennines, Italy. Tectonophysics, 450(1), 34-50.

Vitale Brovarone, A., Herwartz, D., 2013. Timing of HP metamorphism in the Schistes Lustrés of Alpine Corsica: New Lu–Hf garnet and lawsonite ages. Lithos, 172, 175-191.

Vitale Brovarone, A., Beyssac, O., Malavieille, J., Molli, G., Beltrando, M., Compagnoni, R., 2013. Stacking and metamorphism of continuous segments of subducted lithosphere in a high-pressure wedge: the example of Alpine Corsica (France). Earth-Science Reviews, 116, 35-56.

Whitmarsh, R.B., Manatschal, G., Minshull, T.A., 2001. Evolution of magma-poor continental margins from rifting to seafloor spreading. Nature 413, 150-154.

Winterer, E.L., Bosellini, A., 1981. Subsidence and sedimentation on Jurassic passive continental margin, Southern Alps, Italy. AAPG Bulletin 65, 394-421.

Zanchetta, S., Garzanti, E., Doglioni, C., Zanchi, A., 2012. The Alps in the Cretaceous: a doubly vergent pre-collisional orogen. Terra Nova 24, 351-356.

Zarki-Jakni, B., van der Beek, P., Poupeau, G., Sosson, M., Labrin, E., Rossi, P., Ferrandini, J., 2004. Cenozoic denudation of Corsica in response to Ligurian and Tyrrhenian extension: results from apatite fission track thermochronology. Tectonics, 23(1).

Zattin, M., Fellin, M.G., Cavazza, W., Picotti, V., Vance, J.A., Zuffa G.G., 2001. Exhumation of northern Corsica (France). Geophysical Research Abstracts 3, 531.

Zattin, M., Massari, F., Dieni, I., 2008. Thermochronological evidence for Mesozoic-Tertiary tectonic evolution in the Eastern Sardinia. Terra Nova 20, 469-474.

FIGURE CAPTIONS

Figure 1. A: Tectonic map of the Mediterranean area (bottom right) and digital topographic-bathymetric model of Corsica-Sardinia and adjoining basins looking west (after http://www.virtualocean.org; 10/1 vertical exaggeration, location in the inset). The elevation of the wedge-shaped Corsica-Sardinia block gradually decreases from north to south. Note the contrasting physiography between the northern and southern Tyrrhenian basins, and the drastic change in basement lithology across the Central Fault (circles indicate rocks exposed or found by drilling, compiled after Colantoni et al., 1981; Sartori, 1986; Schreider et al., 1986; Bigi et al., 1991; 1992; Sartori et al., 2004).

B: Paleogene evolution of the Western Mediterranean according to the young-Apennines (left) and ancient-Apennines (right) hypotheses (based on Doglioni et al., 1999; Jolivet et al., 2003; Argnani, 2012; Carminati et al., 2012; Molli and Malavieille, 2012). In the former case, Sardinia is located in a lower plate position during most of its evolution, and the northern distal margin of Tethys is subducted beneath the Adriatic plate. In the latter case, Sardinia is located in an upper plate position from the Mesozoic, and the distal Tethyan margin is possibly preserved. Note that paleotectonic reconstructions consistent with the ancient-Apennines hypothesis may locate the Paleogene northern tip of Adriatic subduction either in front of Sardinia (e.g., Argnani et al., 2009) or in front of Corsica (e.g., Jolivet et al., 2003).

Figure 2: Geological sketch map of Corsica-Sardinia (simplified after Carmignani et al., 2000, modified in Corsica according to original field data), showing the location of analyzed samples (large black dots); small dots indicate the location of literature low-T geochronological data from Sardinia (Zattin et al., 2008) and Corsica (Cavazza et al., 2001; Danišík et al., 2007; 2012; Fellin et al., 2005; 2006; Mailhé et al., 1986; Zarkni-Jakni et al., 2004; Zattin et al., 2001), numbers indicate literature ZFT ages from Variscan Corsica.

Figure 3: Conceptual thermochronological model showing a simplified thermal structure (based on Whitmarsh et al., 2001) before and after continental break-up (left), and the corresponding age pattern possibly preserved in the distal passive margin (right). The proximal margin is little affected by rift-

related heating, and the thermochronological record is chiefly controlled by erosion (e.g., Gallagher et al., 1994). In the distal margin, syn-rift sedimentation indicates a minor impact of erosion, and the thermochronological record is possibly controlled by rift-related heating and subsequent thermal relaxation after continental break-up (at time t_B); isothermal surfaces before and after break-up define bell-shaped areas lying at different depths according to their temperature (surfaces in the model roughly correspond to ZFT, AFT and AHe isotopic closure); inside each half-bell, mineral ages are set during thermal relaxation after break-up (age = t_B); below the half-bell, ages are set during late exhumation or younger thermal events (age < t_B); above the half-bell, rocks largely preserve the thermochronological fingerprint acquired before rifting (age > t_B), but a reduction in MTL and slight age rejuvenation are expected in samples that have cooled through the partial annealing zone (PAZ, in red for the AFT system).

On the right, resulting age patterns in the distal passive margin according to crustal level and original distance from the rift axis; close to the rift axis (B), MTL reduction affects thicker crustal sections, and rocks (white circles) may yield indistinguishable ages (= t_B) using different thermochronometers, even in the absence of fast exhumation or magmatic crystallization (cf. Malusà et al., 2011b).

Figure 4. **A:** low-T thermochronological dataset from Sardinia (same key as Fig. 2). AHe, apatite U–Th/He age; AFT, apatite fission-track age; ZFT, zircon fission-track age. Literature AFT data are from Zattin et al. (2008). **B:** Mean track length vs. AFT age relationship in analyzed samples (black dots) as compared to literature data (standard error <0.25 μm not reported).

Figure 5: Mesozoic evolution of Corsica-Sardinia.

A: Trend of crustal isopachs on the northern Tethyan margin, as inferred from available geochronological data interpreted according to the conceptual model in Figure 3 (see text for details).

B: Transect across the northern Tethyan margin shortly after Jurassic rifting. Brown vertical bars show the inferred burial depth of different crustal sections now exposed in Corsica-Sardinia (isothermal surfaces before break-up and after thermal relaxation as in Fig. 3). Burial depth gradually decreases from NW Corsica to SE Sardinia. Rocks exposed in SE Sardinia were already at shallow depth (<1-2 km) in Jurassic times, and close to the rift axis (AFT and AHe ages were set during thermal relaxation at 160-170 Ma, or even earlier). Crustal thickness (not to scale) according to Figure 5A.

C: Transect across the northern Tethyan margin in Cretaceous times after shoulder uplift and post-rift subsidence. The eroded crustal section is shown in light grey, blue lines are faults inferred from

low-T geochronology data (Jurassic isothermal surfaces are kept as marker). Peneplanation in the NW is coeval with marine sedimentation in the SE.

Figure 6: Time-temperature paths, modeled with HeFTy, for block-H samples collected over an elevation range of ~1100 m (cf. Fig. 5B). Modeling is based on AFT age and track length distribution, with no additional external constraint; the best-fit path (thick black line) is only valid inside the partial annealing zone (PAZ), where it is marked by a continuous line; the grey area is the envelope of the good-fit paths (GOF = goodness of fit). Black dots mark the temperature of analyzed samples after rising of isothermal surfaces during rifting: at time t_0, sample S20 lies below the PAZ, samples S19 and S18 lie in the upper part of the PAZ, sample S17 lies above the PAZ. Cooling of samples S17 to S19 is ascribed to erosional exhumation before continental break-up, and is coeval with major Upper Triassic – Lower Jurassic stratigraphic gaps. Cooling of sample S20 is ascribed to thermal relaxation after continental break-up at time t_B, recorded by the AFT system with delays within age uncertainty. These time-temperature paths show that the geothermal gradient dropped from >80°C/km during rifting (t_0), to ~30°C/km during spreading (t_B).

Figure 7. Top-left: AFT ages from Variscan Corsica and Sardinia plotted against distance along a NW-SE transect (N-S in Paleogene coordinates). Mesozoic ages related to Tethyan rifting, Neogene ages along the Sardinia rift, and ages potentially affected by Alpine tectonic burial (i.e., from samples <5 km from the Alpine wedge) are not included. Ages systematically decrease from SE to NW (error bars = 1σ; R is the regression coefficient of the regression line in dashed grey).

Top-right: AFT age vs. mean track length (MTL) diagram for the same samples (error bars as in Fig. 4B). The distribution shows a minimum at 49 Ma, after which MTL steadily increases as AFT age decreases, suggesting progressively faster cooling inside the partial annealing zone (PAZ) towards the NW.

Bottom: Representative time-temperature paths modeled with HeFTy based on AFT age and track length distribution with no additional external constraint (same key as in Fig. 6; grey path in B is additionally constrained by AHe data). Thermal histories are modeled for the last 160 Ma, but are only shown for the last 60 Ma when samples are exhumed across the PAZ. Note the decreasing slope of modeled paths from A to D, which suggests faster cooling inside the PAZ towards the NW. Cooling was diachronous along the transect: sample A entered the PAZ when sample B was already exhumed above the PAZ (like sample B when compared to samples C and D); this is inconsistent with tilting and supportive of an erosional pulse migrating northward during the Paleogene (paths A and B are from Danišík et al., 2007; 2012).

Figure 8: Cenozoic evolution of Corsica-Sardinia (same key as in Fig. 5).

A: The mid-Cretaceous paleosurface is buried beneath Paleogene sediments (thicker towards the NW) and then progressively re-exposed by erosional exhumation. Sedimentary burial led to widespread AFT resetting; AFT data constrain the subsequent erosional pulse, which gets younger from SE (~67 Ma) to NW (~23 Ma) (cf. Fig. 7); detritus produced during exhumation is progressively transferred northward and redeposited on the Variscan basement. Blue lines are faults displacing the mid-Cretaceous paleosurface, thus providing additional accommodation space for the Eocene flysch sequences of northern Corsica (E2 in Fig. 2).

B: Corsica-Sardinia has become an independent continental block bounded by Neogene basins, and is finally tilted. Uplift is higher in NW Corsica (where elevation now exceeds 2700 m a.s.l.) and progressively decreases towards southern Corsica and Sardinia (cf. Fig. 1A), where mantle was exhumed at shallow depth during Tethyan rifting. Paleogene deposits are locally preserved above the tilted mid-Cretaceous paleosurface.

Figure 9: Upper plate response to Adriatic slab motion.

A: 3D model of the Western Mediterranean showing the Adria trajectory relative to Europe between 67 and 23 Ma (grey arrow, from Dewey et al., 1989), and the exhumation trend in Corsica-Sardinia during the Paleogene as constrained by low-T thermochronometers. The large vertical arrows, in color, indicate age and site of erosional exhumation (longer arrows = faster rates); the dashed black arrows indicate the pattern of sediment dispersal.

Relationships between tectonic plates are referred to the late Eocene time frame (35 Ma): on the left side of the model (Corsica transect - CO), choking European subduction beneath Adria is coeval with exhumation of eclogite units (dark blue) at the rear of the frontal Alpine wedge (light blue); on the right side of the model, Adriatic continental crust and Mesozoic oceanic crust (green) are actively subducted beneath Sardinia (SA) and the Baronie Seamount (BS), forming an Apenninic wedge (light blue) also including Calabria (CA). The northward translation of the Adriatic slab beneath Sardinia and Corsica is mirrored by the coeval migration of exhumation pulses at the surface between 49 and 23 Ma.

B: Cartoon showing the linkage between lateral slab translation and migrating erosional pulses on the upper plate; black dots indicate fixed points on the lower (L) and upper (U) plate; transect location as in Figure 10C.

Figure 10: Evolution of the Western Mediterranean since the Cretaceous (Adria trajectories relative to Europe from Dewey et al., 1989; shape of the Adria promontory and enclosed Cretaceous wedge after Malusà et al., 2011a).

A: In mid-Cretaceous time, Sardinia (SA) faces the Southalpine domain (SO); the continental crust isopachs of the European and Adriatic margins (thick dashed lines) are parallel to the major

Variscan faults in the mainland (e.g., Cévennes Fault); between 100 and 80 Ma, Adria moves parallel to the Tethyan passive margin, which is preserved north of the future Central Fault.

B: In the latest Cretaceous, Alpine Tethys is nearly closed by Alpine subduction (the future External Massifs are shown in grey for reference); accretion of Austroalpine units (AU) in the Cretaceous wedge, including the Sesia-Lanzo (SL), is complete; the inherited tectonic configuration south of the Central Fault includes slivers of lower crust now exposed in Calabria.

C: E-W Adria-Europe convergence (67-49 Ma) is accommodated along the Corsica transect by eastward subduction propagating from the Eastern Alps, and along the Sardinia transect by westward subduction possibly propagating from the Betics.

D: Choking of Alpine subduction and localized extension in the Alpine trench in the late Eocene triggers superfast exhumation of the Eclogite belt (Malusà et al., 2011a); Adria subduction is still active to the south, the Adriatic slab starts its northward travel beneath Sardinia.

E: The Adriatic slab shifts farther north beneath the Alpine wedge of Corsica; the onset of slab rollback induces extension in the backarc region; Adriatic foredeep turbidites are progressively accreted within the Apenninic wedge.

F: The Corsica-Sardinia block has completed its counterclockwise rotation and experiences differential uplift; west of the Central Fault, the inheritance of Tethyan rifting is still largely preserved.

Abbreviations: AA, Aar; AG, Argentera; AU, Austroalpine; BS, Baronie Smt; CA, Calabria; CO, Corsica; CT, Cornaglia Terrace; EB, Epiligurian basins; FV, Farinole-Volpajola; MB, Mont Blanc; ME, Maures-Esterel; PE, Pelvoux; SA, Sardinia; SL, Sesia-Lanzo; SO, Southalpine; TE, Tenda; TPB, Tertiary Piedmont Basin; VA, Vavilov.

Supplementary material:

Table S1: AFT data

Table S2: ZFT data

Table S3: AHe data

Table S4: Sample location

Figure S5: Radial plots and histograms of single grain AFT and ZFT ages of samples failing the chi-square test.

Malusà et al. - Figure 1

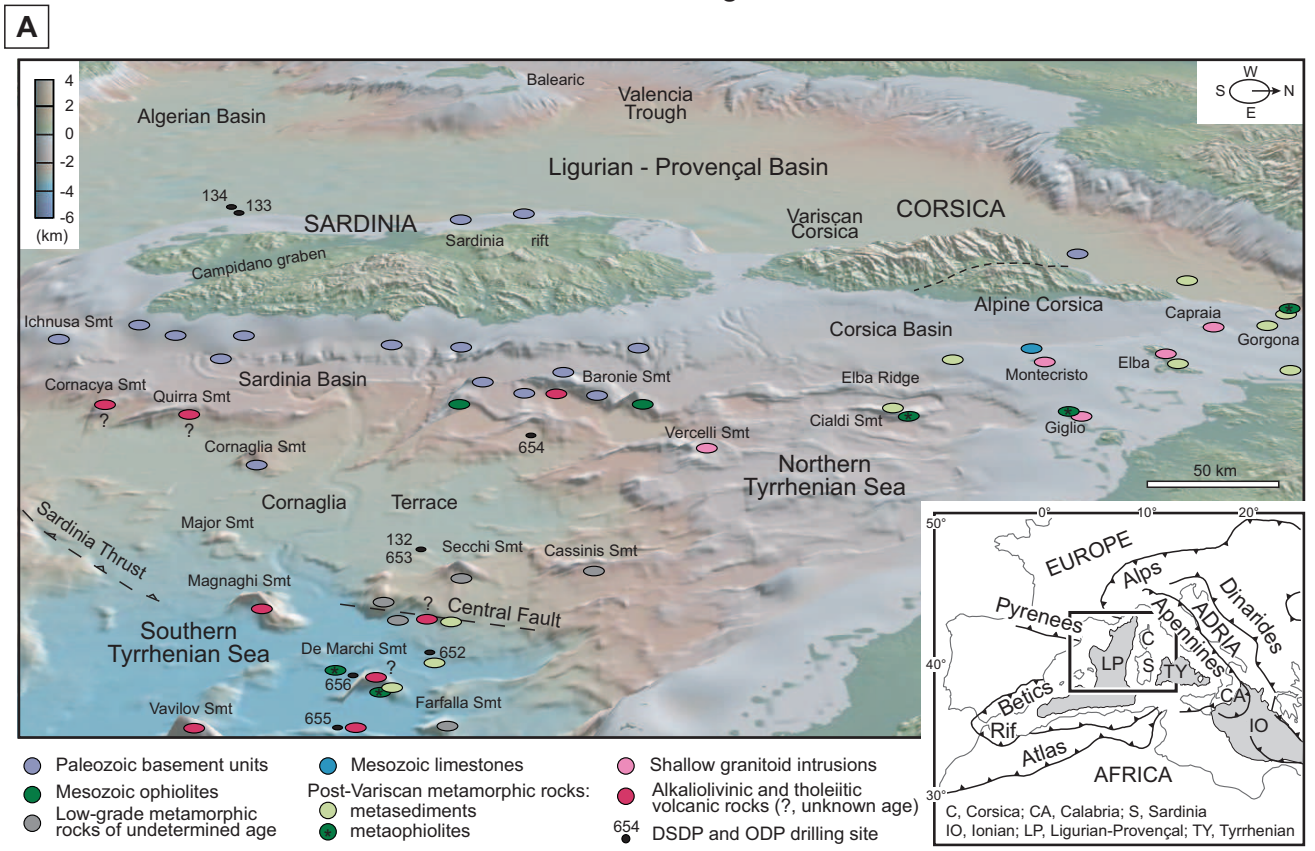

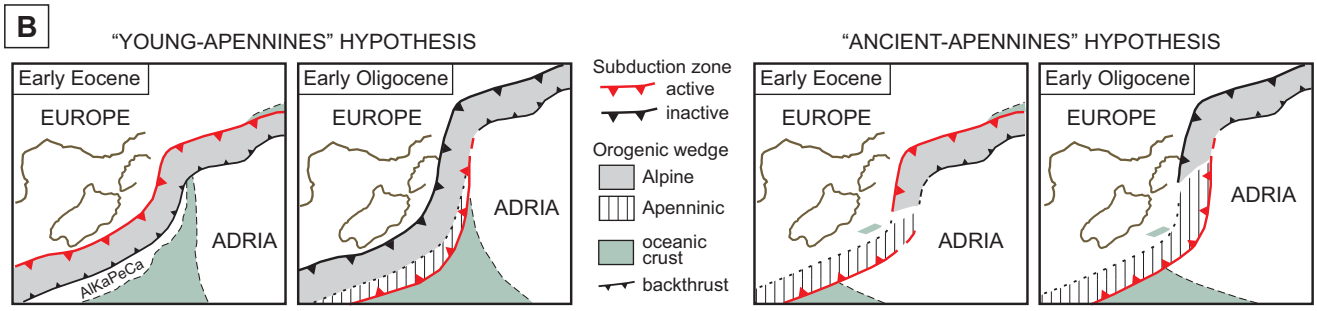

Malusà et al. - Figure 2

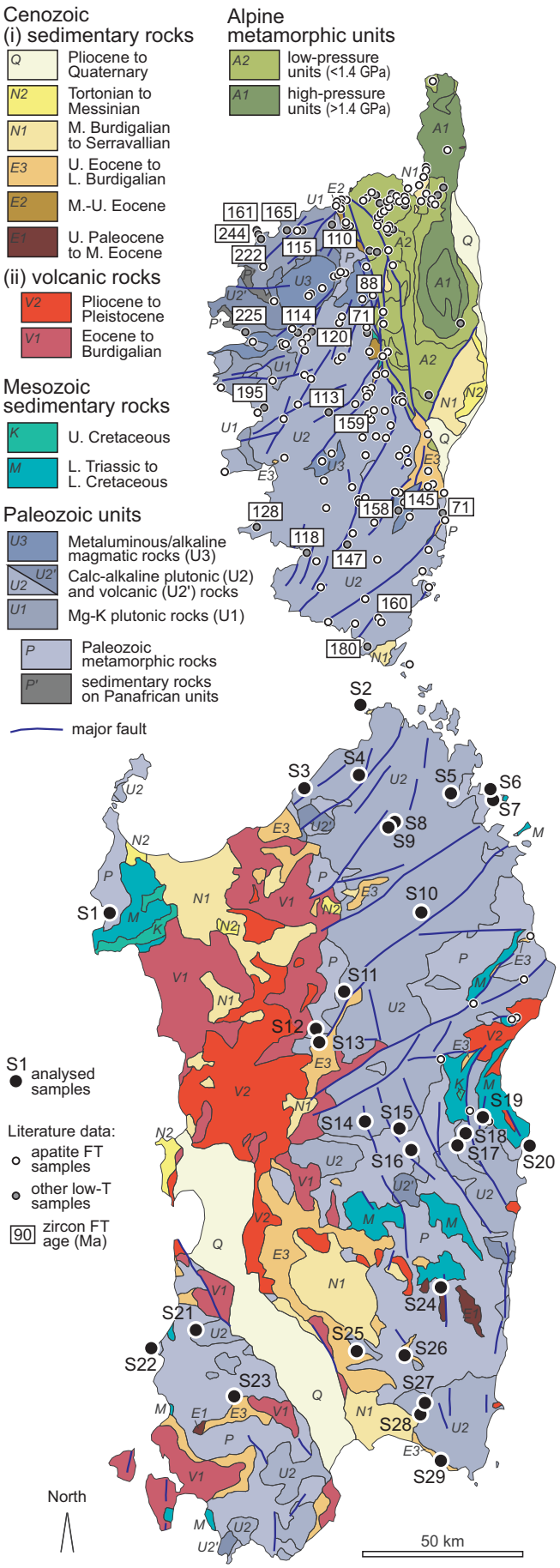

Malusà et al. - Figure 3

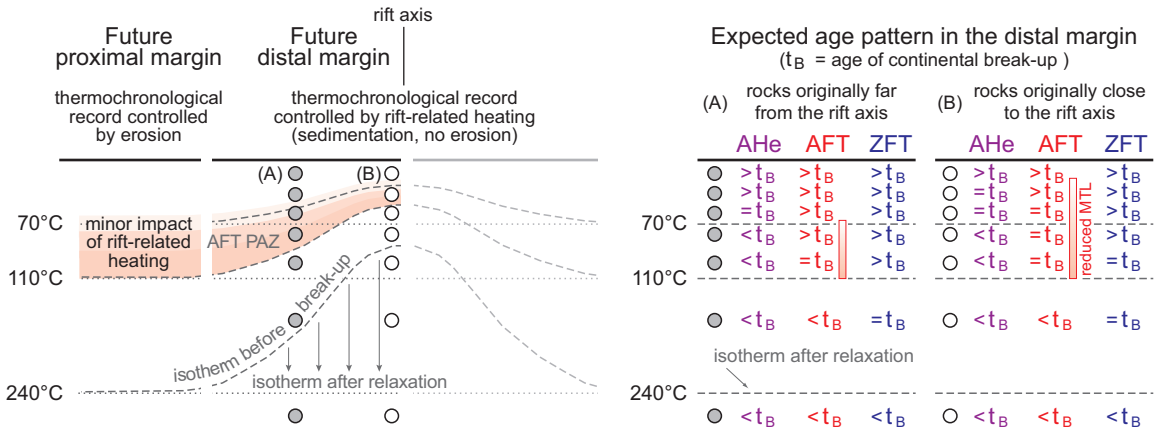

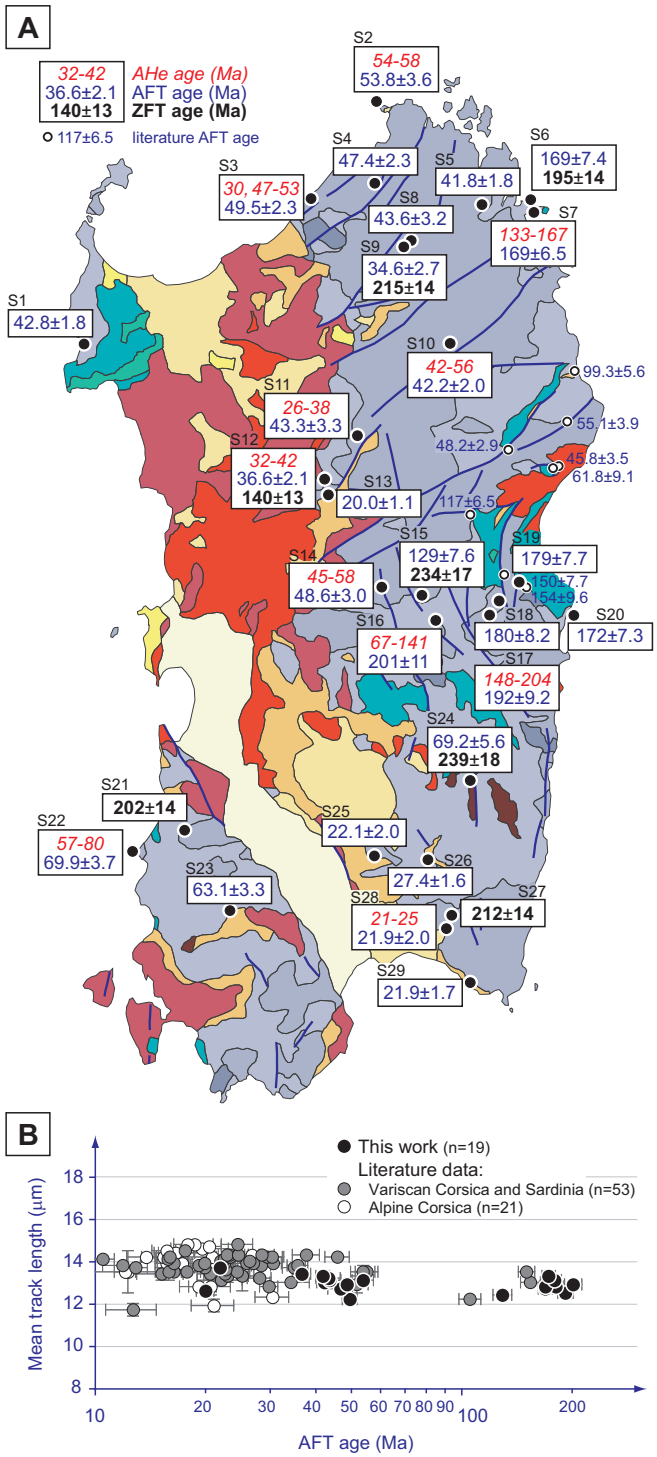
A
32-42
36.6±2.1
140±13
AHe age (Ma)
AFT age (Ma)
ZFT age (Ma)
117±6.5
literature AFT age
S1
42.8±1.8
S2
54-58
53.8±3.6
S3
30, 47-53
49.5±2.3
S4
47.4±2.3
S5
41.8±1.8
S6
169±7.4
195±14
S7
133-167
169±6.5
S8
43.6±3.2
S9
34.6±2.7
215±14
S10
42-56
42.2±2.0
99.3±5.6
S11
26-38
43.3±3.3
55.1±3.9
48.2±2.9
S12
32-42
36.6±2.1
140±13
45.8±3.5
61.8±9.1
S13
20.0±1.1
117±6.5
S14
45-58
48.6±3.0
S15
129±7.6
234±17
S19
179±7.7
150±7.7
154±9.6
S16
67-141
201±11
S18
180±8.2
S20
172±7.3
S17
148-204
192±9.2
S24
69.2±5.6
239±18
S21
202±14
S22
57-80
69.9±3.7
S23
63.1±3.3
S25
22.1±2.0
S26
27.4±1.6
S27
212±14
S28
21-25
21.9±2.0
S29
21.9±1.7
B
This work (n=19)
Literature data:
Variscan Corsica and Sardinia (n=53)
Alpine Corsica (n=21)
Mean track length (µm)
18
16
14
12
10
8
10
20
30
40
50
60
70
80
90
100
200
AFT age (Ma)

Malusà et al. - Figure 5

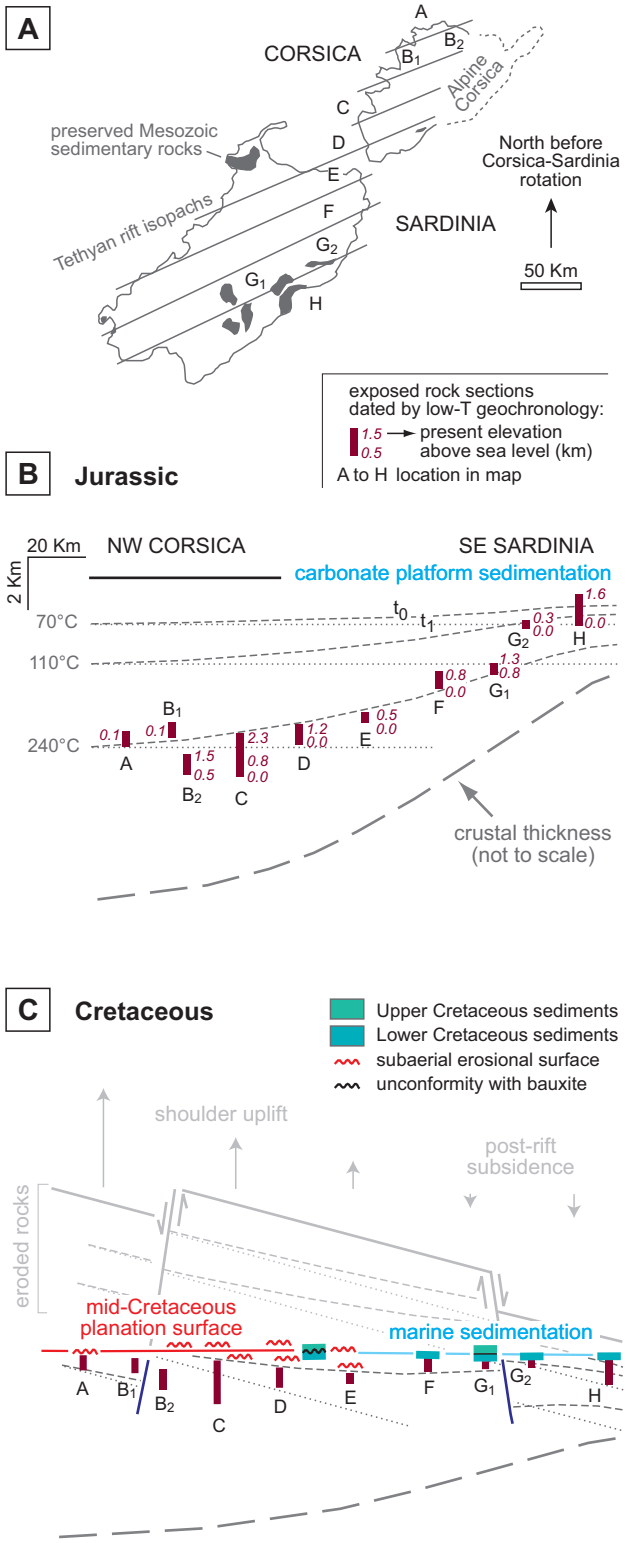

Malusà et al. - Figure 6

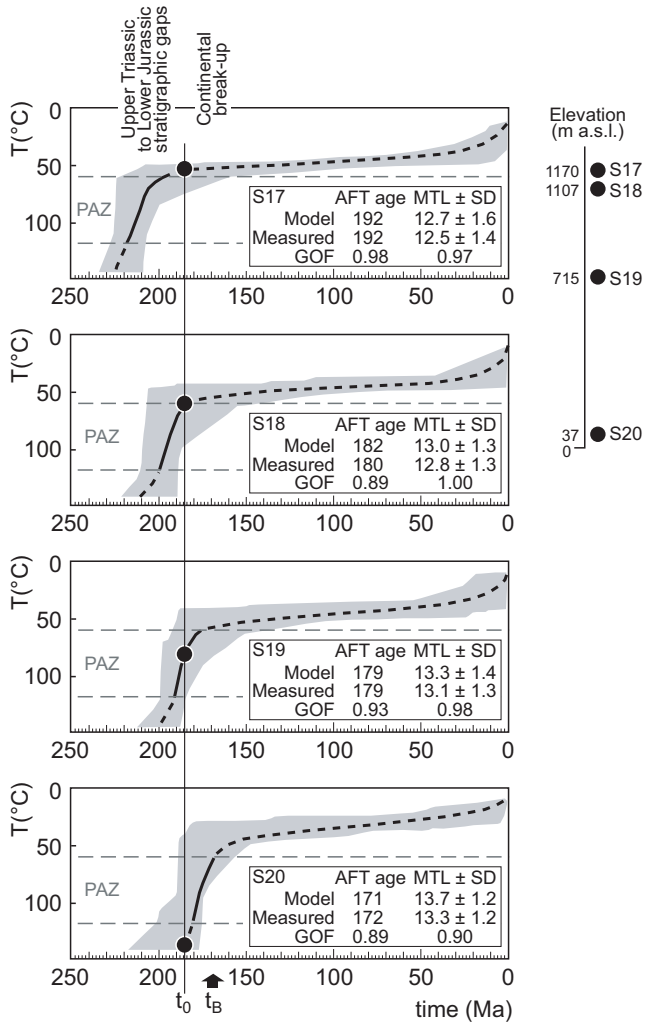

Malusà et al. - Figure 7

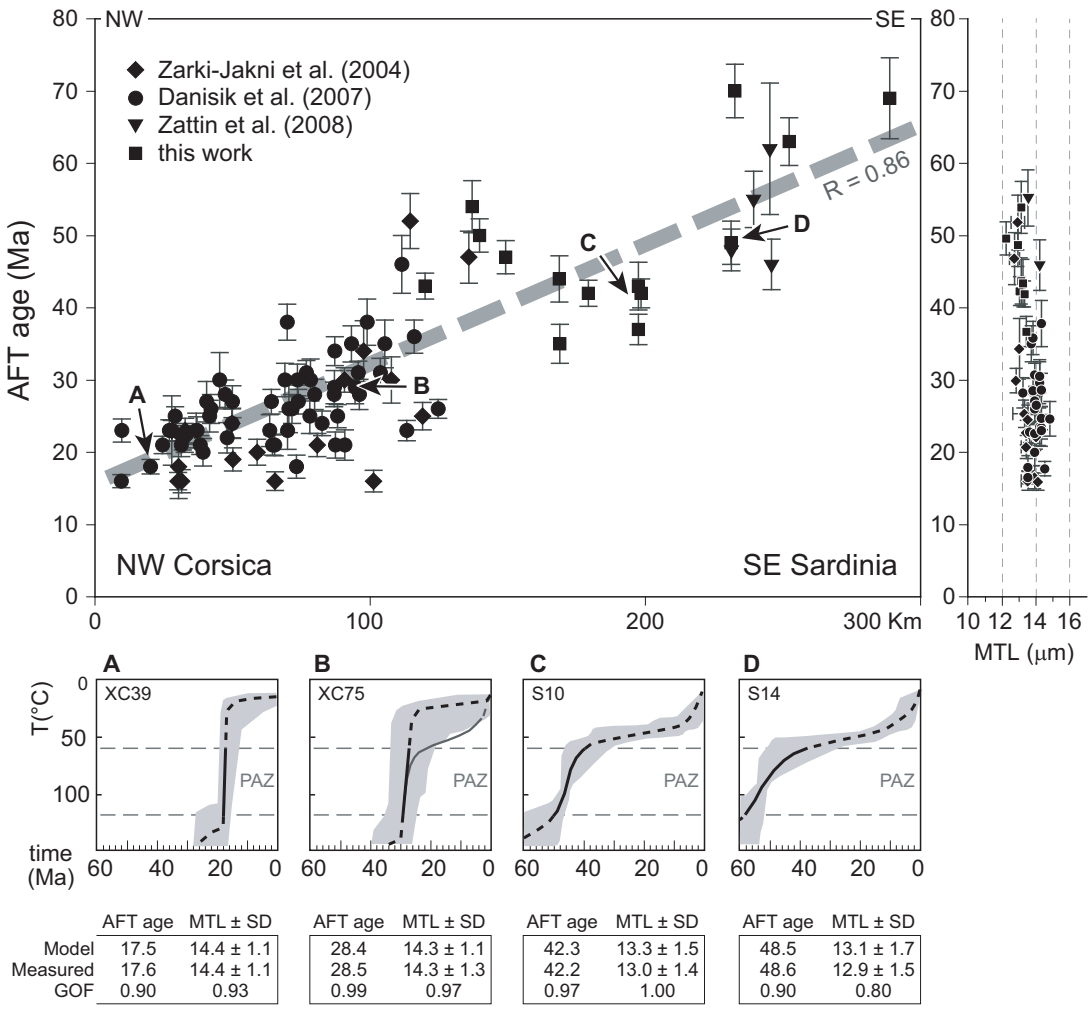

	A		B		C		D	
	AFT age	MTL ± SD	AFT age	MTL ± SD	AFT age	MTL ± SD	AFT age	MTL ± SD
Model	17.5	14.4 ± 1.1	28.4	14.3 ± 1.1	42.3	13.3 ± 1.5	48.5	13.1 ± 1.7
Measured	17.6	14.4 ± 1.1	28.5	14.3 ± 1.3	42.2	13.0 ± 1.4	48.6	12.9 ± 1.5
GOF	0.90	0.93	0.99	0.97	0.97	1.00	0.90	0.80

Malusà et al. - Figure 8

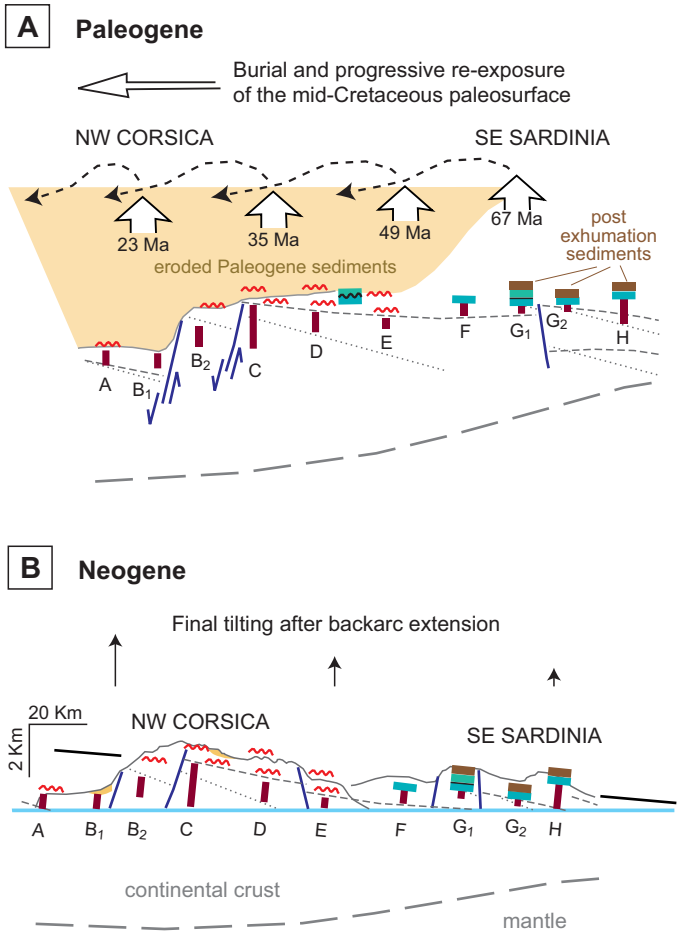

Malusà et al. - Figure 9

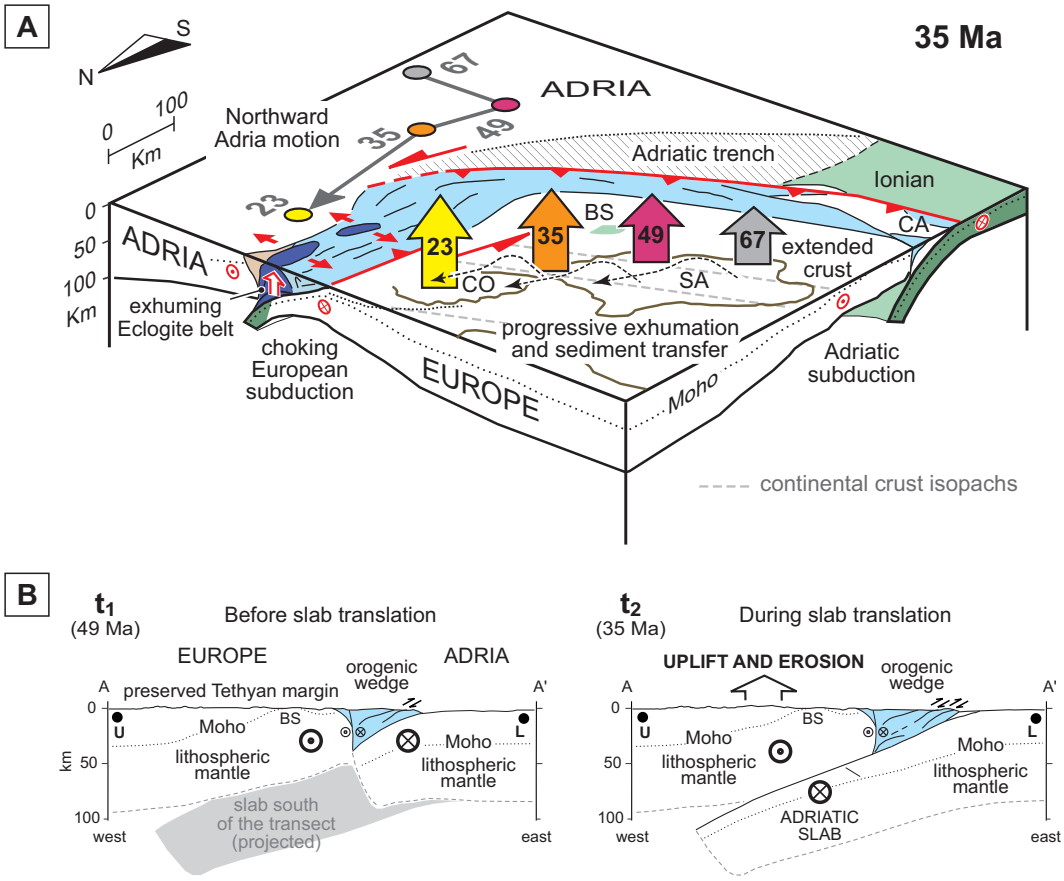

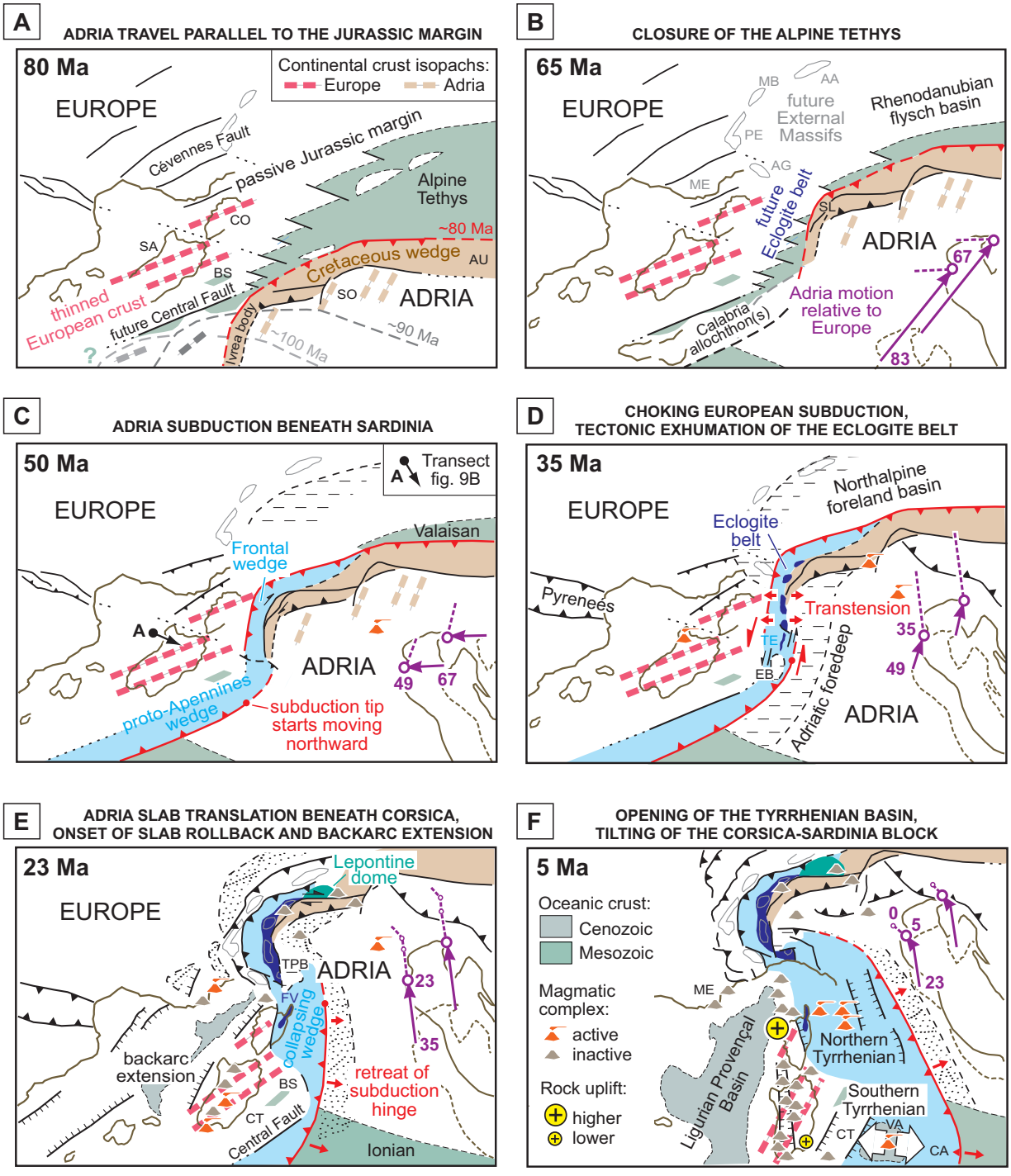
A
ADRIA TRAVEL PARALLEL TO THE JURASSIC MARGIN
80 Ma
Continental crust isopachs:
Europe
Adria
EUROPE
Cévennes Fault
passive Jurassic margin
Alpine Tethys
CO
SA
BS
~80 Ma
Cretaceous wedge
AU
thinned European crust
future Central Fault
SO
ADRIA
Ivrea body
~100 Ma
~90 Ma
?
B
CLOSURE OF THE ALPINE TETHYS
65 Ma
EUROPE
MB
AA
future External Massifs
Rhenodanubian flysch basin
PE
AG
ME
future Eclogite belt
SO
ADRIA
67
Adria motion relative to Europe
Calabria allochthon(s)
83
C
ADRIA SUBDUCTION BENEATH SARDINIA
50 Ma
Transect A fig. 9B
EUROPE
Valaisan
Frontal wedge
A
ADRIA
49
67
proto-Apennines wedge
subduction tip starts moving northward
D
CHOKING EUROPEAN SUBDUCTION, TECTONIC EXHUMATION OF THE ECLOGITE BELT
35 Ma
EUROPE
Northalpine foreland basin
Eclogite belt
Pyrenees
Transtension
TE
35
49
EB
Adriatic foredeep
ADRIA
E
ADRIA SLAB TRANSLATION BENEATH CORSICA, ONSET OF SLAB ROLLBACK AND BACKARC EXTENSION
23 Ma
EUROPE
Lepontine dome
TPB
ADRIA
23
FV
collapsing wedge
35
backarc extension
BS
retreat of subduction hinge
CT
Central Fault
Ionian
F
OPENING OF THE TYRRHENIAN BASIN, TILTING OF THE CORSICA-SARDINIA BLOCK
5 Ma
Oceanic crust:
Cenozoic
Mesozoic
Magmatic complex:
active
inactive
Rock uplift:
higher
lower
0
5
23
ME
Northern Tyrrhenian
Ligurian Provençal Basin
Southern Tyrrhenian
CT
VA
CA